Journal of Alzheimer's Disease 34 (2013) 1015–1035
DOI 10.3233/JAD-121750
IOS Press

Cortical Sources of Resting State EEG Rhythms are Sensitive to the Progression of Early Stage Alzheimer's Disease

Claudio Babiloni[a,b,*], Roberta Lizio[b], Claudio Del Percio[b], Nicola Marzano[c], Andrea Soricelli[c,d], Elena Salvatore[e], Raffaele Ferri[f], Filomena I.I. Cosentino[f], Gioacchino Tedeschi[e], Patrizia Montella[e], Silvia Marino[g], Simona De Salvo[g], Guido Rodriguez[h], Flavio Nobili[h], Fabrizio Vernieri[i], Francesca Ursini[i], Ciro Mundi[j], Jill C. Richardson[k], Giovanni B. Frisoni[l] and Paolo M. Rossini[b,m]
[a]*Department of Molecular Medicine, University of Rome "Sapienza", Rome, Italy*
[b]*IRCCS San Raffaele Pisana, Roma, Italy*
[c]*IRCCS "SDN", Naples, Italy*
[d]*Department of Studies of Institutions and Territorial Systems, University of Naples Parthenope, Naples, Italy*
[e]*Department of Neurological Sciences, University of Naples Federico II, Naples, Italy*
[f]*IRCCS Oasi, Troina (Enna), Italy*
[g]*SICILIA- IRCCS Centro Neurolesi "Bonino-Pulejo" – Messina, Italy*
[h]*Service of Clinical Neurophysiology (DiNOG; DipTeC), Hospital-University of Genoa S. Martino, Genoa, Italy*
[i]*Neurology, University "Campus Biomedico", Rome, Italy*
[j]*Department of Neuroscience, United Hospitals of Foggia, Foggia, Italy*
[k]*GlaxoSmithKline R&D China Group, Gunnels Wood Road, Stevenage, Hertfordshire, UK*
[l]*IRCCS "S. Giovanni di Dio-FBF.", Brescia, Italy*
[m]*Department of Geriatrics, Neuroscience and Orthopedics, Institute of Neurology Catholic University "Sacro Cuore" Rome, Italy*

Handling Associate Editor: J. Wesson Ashford

Accepted 21 December 2012

Abstract. Cortical sources of resting state electroencephalographic (EEG) rhythms are abnormal in subjects with Alzheimer's disease (AD). Here we tested the hypothesis that these sources are also sensitive to the progression of early stage AD over the course of one year. The resting state eyes-closed EEG data were recorded in 88 mild AD patients at baseline (Mini Mental State Evaluation, MMSE I = 21.7 ± 0.2 standard error, SE) and at approximately one-year follow up (13.3 months ± 0.5 SE; MMSE II = 20 ± 0.4 SE). All patients received standard therapy with acetylcholinesterase inhibitors. EEG recordings were also performed in 35 normal elderly (Nold) subjects as controls. EEG rhythms of interest were delta (2–4 Hz), theta (4–8 Hz), alpha 1 (8–10.5 Hz), alpha 2 (10.5–13 Hz), beta 1 (13–20 Hz), beta 2 (20–30 Hz), and gamma (30–40 Hz). Cortical EEG sources were estimated by low-resolution brain electromagnetic tomography (LORETA). Compared to the Nold subjects, the mild AD patients were characterized by a power increase of widespread delta sources and by a power decrease of posterior alpha sources. In the mild AD patients, the follow-up EEG recordings showed increased power of widespread delta sources as well as

*Correspondence to: Prof. Claudio Babiloni, Ph.D., Department of Molecular Medicine, University of Rome "Sapienza", P.le A. Moro 5, Rome I-00185, Italy. Tel./Fax: +39 06 49910989 0917; E-mail: claudio.babiloni@uniroma1.it.

ISSN 1387-2877/13/$27.50

decreased power of widespread alpha and posterior beta 1 sources. These results suggest that the resting state EEG sources were sensitive, at least at group level, to the cognitive decline occurring in the mild AD group over a one-year period, and might represent cost-effective and non-invasive markers with which to enrich cohorts of AD patients that decline faster for clinical studies.

Keywords: Alzheimer's disease, disease progression, electroencephalography, low resolution brain electromagnetic tomography (LORETA)

INTRODUCTION

Alzheimer's disease (AD) is an irreversible disorder characterized by a progressive neuronal deterioration resulting in a loss of cognitive functions [1]. Therefore, it is of great interest to define instrumental markers of the disease progression, namely those sensitive to the progression of the cognitive dysfunction in AD patients over time.

Nowadays, several instrumental markers are available for the assessment of AD patients [2–6]. They include the analysis of cerebrospinal fluid (CSF) sampled by lumbar puncture measuring amyloid-β (Aβ) and tau metabolites as key indicators of pathology [7]. Structural magnetic resonance imaging (MRI) detects neurodegeneration in the brain as measured by regional atrophy of the hippocampus and cerebral cortex [8–12]. Resting state positron emission tomography (PET)-fluoro-deoxy-glucose (FDG) allows the mapping of typical temporo-parietal, posterior cingulate, and precuneous hypometabolism in AD patients [13, 14]. Furthermore, PET-amyloid Pittsburg Compound B (PIB) is used for the visualization *in vivo* of Aβ deposition in the brain of AD patients [15–17]. However, all of these instrumental markers are relatively expensive and invasive, and cannot be systematically applied to all AD patients. Specifically, with the need to perform drug studies in the pre-clinical or at-risk population, there is a major requirement for the AD scientific community to develop novel non-invasive and relatively cheap markers that accurately reflect the progression of AD pathology.

Previous studies in AD patients have shown that the power (i.e., spectral power density) of resting state eyes-closed electroencephalographic (EEG) rhythms might provide promising markers of the disease state [18–23]. It has been reported that compared to normal elderly (Nold) subjects, AD patients are characterized by higher power of widespread delta (0–3 Hz) and theta rhythms (4–7 Hz), lower power of posterior alpha rhythms (8–12 Hz) with a slowing of the alpha peak frequency, and lower power of beta (14–30 Hz) and gamma (around 40 Hz) rhythms [19, 24–31]. Only a few studies have reported a difference of resting EEG power at gamma band (around 40 Hz) between Nold and mild AD with contrasting results. One study reported lower power of gamma (35–45 Hz) rhythms in AD compared to Nold subjects [32]; on the contrary, another study showed an increase of gamma (30–70 Hz) rhythms in AD compared to Nold subjects [33]. The more reproducible EEG abnormalities (i.e., ratio of alpha/delta global field power) were associated with markers of the amyloid cascade measured in the CSF of AD subjects [34]. Furthermore, they were associated with altered resting state regional cerebral blood flow (rCBF), as measured by single photon emission computerized tomography or PET-FDG [35, 27], and with the severity of the cognitive impairment in AD patients, as indexed by Mini Mental State Examination (MMSE) score [35].

The functional significance of EEG abnormalities in AD is further evidenced by studies investigating the relationship between EEG rhythms and cognition in humans (i.e., attention, memory). It has been shown that a good cognitive performance is predicted by high alpha power and low theta power in the pre-stimulus period [36, 37]. Successful encoding processes would depend on the increase of the frontal theta power, reflecting the functional mode of loops including basal forebrain, hippocampus, and cerebral cortex [36, 37]. Later, successful retrieval processes into semantic or episodic long-term memory would depend on the decrease of posterior alpha power, reflecting the functional mode of thalamo-cortical and cortico-cortical feedback loops [36]. As a general rule, the stronger the pre-stimulus alpha power, the stronger its power reduction during the stimulus processing, and the better the cognitive performance [36, 37]. A relationship between power of EEG rhythms and cognition was also found in AD and in mild cognitive impairment (MCI) subjects [38–40]. In particular, the power of alpha rhythms was positively related to global cognitive status (i.e., MMSE score), immediate memory for digits probing focused attention, and verbal

memory recall [38–40]. On the contrary, the power of delta and theta rhythms was negatively related to global cognition status, visuo-spatial immediate memory probing focused attention, verbal memory recall, and visuo-spatial memory recall [38–40]. Finally, it has been reported that acetylcholinesterase inhibitors (i.e., donepezil, rivastigmine) improve cognitive status (i.e., MMSE and ADAS-Cog), cognitive function, and participation in activities of daily living in patients with mild to moderately severe AD [41–48]. The improvement of the global cognitive status was related to an increase of alpha rhythms or/and decrease of pathological delta rhythms [41, 47, 48].

Only a few "longitudinal" studies in relatively small groups of AD patients have tested the hypothesis that the resting state scalp EEG rhythms could be used as a marker of the disease progression [49–51]. In one study, 27 MCI subjects were followed for a mean period of 21 months between baseline and follow up EEG recordings [51]. At the follow up, the MCI subjects showed a power increase of theta and delta rhythms in temporal and occipital scalp regions and a power decrease of beta rhythms. In another study, a group of 40 AD patients was followed for a mean period of about 30 months between baseline and follow up EEG recordings [49]. At the follow up, the AD patients showed a power increase of theta and delta rhythms in parietal and occipital scalp regions correlating with a power reduction of alpha and beta rhythms [49]. A third longitudinal study was performed in 40 patients followed for a mean period of 12 months [50]. About half of these subjects presented a power increase of theta and delta rhythms in temporal and occipital scalp regions [50]. A methodological limitation of these studies is that the scalp topography of EEG activity is affected by reference electrode and head volume conduction effects, which prevent a precise spatial analysis of EEG rhythms.

Cortical sources of scalp EEG rhythms have been successfully evaluated in AD patients by single dipole sources deeply located into a spherical brain model [24]. Single dipole sources of alpha or beta rhythms were located more anteriorly in AD than in MCI and healthy control subjects [19, 24]. However, model misspecification poses a major problem for dipole source localization as it causes insidious multiple-generator errors to occur in the fitted dipole parameters [52]. An alternative approach for the cortical sources of scalp EEG rhythms is low resolution brain electromagnetic tomography (LORETA) [53], which uses thousands of dipole sources within a 3-D brain model co-registered into Talairach space [54]. With respect to the dipole modeling of cortical sources, no *a priori* decision of the dipole position is required by the investigators in LORETA estimation. LORETA is a promising technique for research in AD since (i) it is freeware, and can be freely downloaded by any research unit worldwide enabling the control/replication of the results for future scientific and clinical applications; and (ii) it has been successfully used in research on AD and EEG markers by independent research groups worldwide [25, 38, 39, 41, 55–72]. In particular, our previous studies have shown that: 1) the posterior sources of dominant alpha rhythms (about 8–10 Hz) were abnormal in AD subjects when compared to Nold, cerebrovascular dementia, and Parkinson disease subjects [55, 69]; 2) the posterior sources of delta (<4 Hz) and dominant alpha rhythms were related to global cognitive status (i.e., MMSE score) in both MCI and AD subjects [38]; 3) the atrophy of hippocampus and cortical gray matter was related to the decline of posterior cortical sources of dominant alpha rhythms in MCI and/or AD subjects [64, 71]; 4) 1-year treatment with an acetylcholinesterase inhibitor (i.e., donepezil) slowed the decline of the posterior cortical sources of dominant alpha rhythms in the 'drug responder group' [41]; and 5) the posterior cortical sources of the dominant alpha rhythms were related to the stability of the global cognitive status in MCI subjects [70].

To our knowledge, previous "longitudinal" studies did not explore whether cortical sources of resting state EEG rhythms can be used as instrumental surrogate markers of the disease progression. These markers may be extremely useful when applied to clinical studies to understand the neurophysiological mechanisms of action of drugs being developed for AD. In the present study, we hypothesized that cortical sources of resting state EEG rhythms were sensitive to both disease state (i.e., cortical sources of resting state EEG rhythms are different between Nold and AD subjects) and progression (i.e., cortical sources of resting state EEG rhythms deteriorate with progression of the disease) in a large cohort of mild AD patients. To test this hypothesis, resting state eyes-closed EEG data were recorded in a large cohort of mild AD patients at baseline (Recording I) and after a mean period of about 1 year (1-year follow up; Recording II). Cortical sources of the EEG rhythms were estimated by means of the LORETA freeware [53], following the procedures reported in the aforementioned reference EEG studies [38, 41, 55, 64, 69–71]. Global cognitive status over time was indexed by the MMSE score [73].

METHODS

We have previously and extensively described the EEG procedures of subjects' recruitment, EEG recording, and LORETA source analysis used in the current study, and part of the present individual data sets was used for previous physiological and pathological aging studies on EEG rhythms [38, 39, 41, 55–71]. In particular, the EEG recording of 100% of Nold and about 40% of mild AD was taken from our "historical" EEG database. About 60% of the new individual EEG data sets of mild AD subjects were recorded and analyzed for the present study. We selected individual data of mild AD subjects from our archive on the basis of the following criteria: (i) fitting with the mentioned inclusion/exclusion criteria; (ii) availability of the EEG recordings and the MMSE scores recorded at baseline time (Recording I; MMSE I) and approximately after 1 year (Recording II; MMSE II) from the first recording; and (iii) MMSE score at baseline between 17–25. Furthermore, we selected individual data sets of Nold subjects matched for age, gender, and education with the mild AD group.

Subjects and diagnostic criteria

For the present multi-centric study, 88 mild AD patients were enrolled. All patients followed a standard daily therapy with an acetylcholinesterase inhibitor (donepezil; 5–10 mg per day; rivastigmine 3 mg per day). We also recruited 35 cognitively normal elderly subjects (Nold) matched for age, gender, and education to serve as controls with the mild AD group.

All experiments were performed with the informed consent of each participant or caregiver, in line with the Code of Ethics of the World Medical Association (Declaration of Helsinki).

Probable AD was diagnosed according to NINCDS-ADRDA [74] and DSM IV criteria. The recruited mild AD patients underwent general medical, neurological, and psychiatric assessments. Patients were also rated with a number of standardized diagnostic instruments that included MMSE [73], Clinical Dementia Rating Scale (CDR) [75], Geriatric Depression Scale (GDS) [76], Hachinski Ischemic Score (HIS, [77]), and Instrumental Activities of Daily Living scale (IADL) [78]. Neuroimaging diagnostic procedures (MRI) and complete laboratory analyses were carried out to exclude other causes of progressive or reversible dementias, in order to enrich for a clinically homogenous mild AD patient group. Exclusion criteria included, in particular, any evidence of (i) frontotemporal dementia, diagnosed according to criteria of Lund and Manchester Groups (1994), (ii) vascular dementia, diagnosed according to NINDS-AIREN criteria [79], (iii) extra-pyramidal syndromes, (iv) reversible dementias (including pseudodementia of depression); and (v) Lewy body dementia. Importantly, benzodiazepines, antidepressant, and/or antihypertensive were suspended for about 24 h before EEG recordings. The control group of Nold subjects was recruited mainly among non-consanguineous relatives of mild AD patients. All Nold subjects underwent physical and neurological examinations as well as cognitive screening (including MMSE and GDS). Subjects affected by chronic systemic illnesses (e.g., diabetes mellitus) were excluded, as were subjects receiving psychoactive drugs. Subjects with a history of present or previous neurological or psychiatric disease were also excluded. All Nold subjects had a GDS score lower than 14 (no depression).

EEG recordings

Resting state eyes-closed EEG data were recorded in the Nold and mild AD subjects by specialized clinical units, in the framework of the diagnostic phase. The EEG recordings were carried out (0.3–70 Hz bandpass) from 19 electrodes positioned according to the International 10–20 System (i.e., Fp1, Fp2, F7, F3, Fz, F4, F8, T3, C3, Cz, C4, T4, T5, P3, Pz, P4, T6, O1, O2; see Fig. 1). A specific kind of reference electrode was not used in all recording units, given that

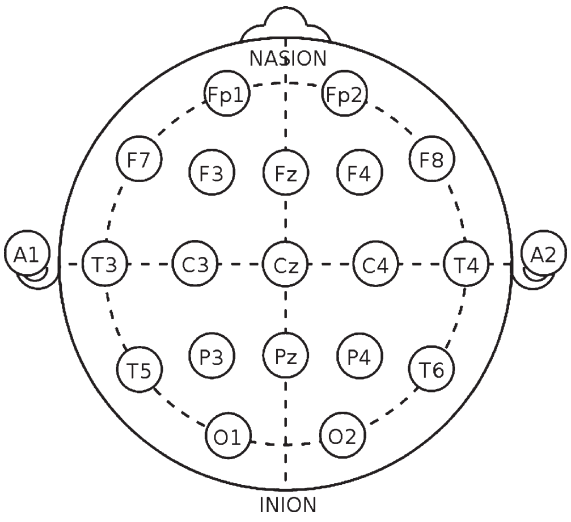

Fig. 1. Recording sites of the 19 scalp electrodes positioned according to the International 10–20 System (i.e., Fp1, Fp2, F7, F3, Fz, F4, F8, T3, C3, Cz, C4, T4, T5, P3, Pz, P4, T6, O1 and O2).

the present preliminary data analysis and LORETA source analysis were based on common average reference. To monitor eye movements, the horizontal and vertical electro-oculogram (0.3–70 Hz bandpass) was also collected. All data were digitized in continuous recording mode (5 min of EEG; 128–256 Hz sampling rate). The EEG data, together with the MMSE scores, were recorded at baseline time (Recording I; MMSE I) and approximately after 1 year (13.3 months ± 0.5 standard error, SE; Recording II; MMSE II) from the first recording. All recordings were performed in the late morning. In order to keep a constant level of vigilance, an on-line experimenter monitored the subject and the EEG traces. He verbally alerted the subject any time there were signs of behavioral and/or EEG drowsiness or the subject opened the eyes. The duration and all other technical characteristics of the EEG recording (5 min) allowed the comparison of the present results with several previous AD studies using either EEG recording periods shorter than 5 min [38, 39, 41, 55–71, 79–82] or about 1 min [24, 25]; longer epochs would have reduced data variability but increased risks for dropping vigilance and arousal.

Preliminary EEG-EOG data analysis

The recorded EEG data were analyzed and segmented off-line in consecutive epochs of 2 s. The EEG epochs with ocular, muscular, and other types of artifact were preliminary identified by a computerized automatic procedure. The EEG epochs with sporadic blinking artifacts (less than 10% of the total) were corrected by an autoregressive method [83]. Two independent experimenters blind to the diagnosis manually confirmed the EEG segments that were acceptable for further analysis. Special attention was given to avoid the inclusion of EEG segments and individual data sets with EEG signs of drowsiness or pre-sleep stages. Finally, we re-referenced off-line artifact free EEG data to a common average for further analysis.

Spectral analysis of the EEG data

A digital FFT-based power spectrum analysis (Welch technique, Hanning windowing function, no phase shift) computed power density of the EEG rhythms with 0.5 Hz frequency resolution. The standard frequency bands of interest were delta (2–4 Hz), theta (4–8 Hz), alpha 1 (8–10.5 Hz), alpha 2 (10.5–13 Hz), beta 1 (13–20 Hz), beta 2 (20–30 Hz), and gamma (30–40 Hz). These band frequencies were chosen averaging those used in a lot of previous relevant EEG studies on dementia, while sharing of a frequency bin by two contiguous bands is a widely accepted procedure [36, 38, 39, 41, 55–71, 73, 84–95]. However, it should be noted that the choice of fixed bands did not account for EEG markers such as individual alpha frequency (IAF) peak, defined as the frequency associated with the strongest EEG power at the extended alpha range [36]. The mean IAF peak, for the mild AD patients, was 8.7 Hz (±0.2 SE) for the Recording I and 8.4 Hz (±0.2 SE) for the Recording II, and for the Nold subjects, was 9.6 Hz (±0.2 SE). Two statistical analyses (ANOVA) were performed to test possible differences in the IAF peak, the first between the Nold and mild AD subjects (at Recording I), and the second, in the mild AD patients, after one year. Statistically significant ANOVA differences were found both using the factor Group (AD- Recording I-, Nold; independent variable; $p < 0.01$) and using the factor Condition (Recording I, Recording II; dependent variable; $p < 0.05$). To control for the residual effect of IAF on the comparison of EEG variables, the IAF peak was used as a covariate (together with age, gender, and education) for further statistical analysis.

We could not use narrow frequency bands for beta 1 (13–20 Hz), beta 2 (20–30 Hz), and gamma (30–40 Hz) bands because of the variability of beta and gamma peaks in the power spectra. Therefore, LORETA results for the beta and gamma bands could suffer from the limitation of sensitivity of EEG spectral analyses for large bands [96].

Cortical source of EEG rhythms as computed by LORETA

The LORETA software as provided at http://www.unizh.ch/keyinst/NewLORETA/LORETA01.htm was used for the estimation of cortical sources of EEG rhythms [53, 97, 98]. LORETA is a source reconstruction technique belonging to a family of linear inverse solution procedures modeling 3D distributions of EEG sources [98]. It has been shown that LORETA was quite efficient when compared to other linear inverse algorithms like minimum norm solution, weighted minimum norm solution or weighted resolution optimization [97–99]. LORETA can be used from EEG data collected by low spatial sampling of 19-electrodes 10–20 system montage, when cortical sources are estimated from resting EEG rhythms [38, 39, 41, 55, 56–71, 73, 100–103]. Furthermore, it has been successfully used by independent research groups in recent EEG studies on AD using the same experimental set

up of the present one [25, 38–41, 55–73]. Noteworthy, this electrode montage is considered as an adequate EEG spatial sampling for the estimation of cortical sources of eyes closed resting state EEG rhythms, since these rhythms are widely represented across all human cerebral cortex in contrast to the circumscribed functional topography of event-related EEG changes (especially at high frequencies) that occur in response to specific sensory or motor events. Therefore, eyes closed resting state EEG rhythms can be properly sampled with a relatively low amount of electrodes, as opposed to the higher spatial sampling required to take into account to the detailed functional topography of event-related EEG activity. This relatively low-spatial sampling of EEG rhythms is consistent with the fact that LORETA solutions are intrinsically maximally smoothed at source space, due to its regularization procedure [53]. LORETA computes 3D linear solutions (LORETA solutions) for the EEG inverse problem within a 3-shell spherical head model including scalp, skull, and brain compartments. The brain compartment is restricted to the cortical grey matter/hippocampus of a head model co-registered to the Talairach probability brain atlas and digitized at the Brain Imaging Center of the Montreal Neurological Institute [104]. This compartment includes 2394 voxels (7 mm resolution), each voxel containing an equivalent current dipole. EEG electrode positions were not co-registered to individual brain source models; unfortunately, the official LORETA package did not include software to do so and we could not obtain the digitalization of the electrode position from our clinical units.

LORETA solutions consisted of voxel z-current density values able to predict EEG spectral power density at scalp electrodes, being a reference-free method of EEG analysis, in that one obtains the same LORETA source distribution for EEG data referenced to any reference electrode, including common average. A normalization of the data was obtained by normalizing the LORETA current density at each voxel with the power density averaged across all frequencies (0.5–45 Hz) and across all 2,394 voxels of the brain volume. After normalization, the solutions lost the original physical dimension and were represented by an arbitrary unit scale. The general procedure fitted the LORETA solutions in a Gaussian distribution and reduced inter-subject variability [87, 105]. Of note, other methods of normalization using the principal component analysis are effective for estimating the subjective global factor scale of the EEG data [106]. These methods are not available in the LORETA package, so they were not used in this study.

Solutions of the EEG inverse problem are underdetermined when the number of spatial samples (electrodes) is lower than the number of the unknown samples (current density at each voxel). To address this, the cortical LORETA solutions predicting scalp EEG spectral power density were regularized to estimate distributed rather than punctate EEG source patterns [53, 97, 98]. In line with the low spatial resolution of the adopted technique, we used our MATLAB software to average LORETA solutions across all voxels of a given cortical macroregion of interest (ROI), i.e., frontal, central, parietal, occipital, and temporal regions of the brain model (Table 1 lists the ROIs in terms of Brodmann areas as defined within the LORETA source space). This methodological option may minimize the effects of poor LORETA estimates in deep voxels (i.e., including those of the limbic region) at which the estimation of EEG sources could be imprecise, especially using an EEG spatial sampling from 19 electrodes (10–20 system).

Finally, the main advantage of the regional analysis of LORETA solutions was that our modeling could disentangle rhythms of contiguous cortical areas. For example, the rhythms of the occipital source were disentangled with respect to those of the contiguous parietal and temporal sources, etc. This was made possible by the fact that LORETA solves the linear inverse problem by taking into account the well-known effects of the head as a volume conductor. With respect to other procedures of data reduction, this type of regional approach may represent an important reference for multimodal comparisons with structural and functional neuroimaging methods (SPECT, PET, surface EEG/MEG topography). Finally, it can be stated that the present approach represents a clear methodological improvement compared to surface electrodes EEG spectral analyses.

Statistical analysis of the LORETA solutions

Regional normalized LORETA solutions from mild AD and Nold subjects were used as a dependent

Table 1
Brodmann areas included in the cortical regions of interest (ROIs) of the present study. LORETA solutions were collapsed in frontal, central, parietal, occipital, and temporal ROIs

LORETA Brodmann Areas into the Regions of Interest	
Frontal	8, 9, 10, 11, 44, 45, 46, 47
Central	1, 2, 3, 4, 6
Parietal	5, 7, 30, 39, 40, 43
Temporal	20, 21, 22, 37, 38, 41, 42
Occipital	17, 18, 19

variable for ANOVA designs using subjects' age, education, gender, and IAF peak as covariates. Mauchly's test evaluated the sphericity assumption. Correction of the degrees of freedom was made with the Greenhouse-Geisser procedure. Duncan test was used for *post-hoc* comparisons ($p < 0.05$). In particular, two ANOVA designs were used to address the main scientific issues of the study.

The first ANOVA design compared the spatial distribution of resting state EEG sources between the Nold and mild AD groups, using the regional LORETA solutions as a dependent variable. The ANOVA factors (levels) were Group (Nold, mild AD; independent variable), Region of interest (central, frontal, parietal, occipital, temporal), and Band (delta, theta, alpha 1, alpha 2, beta 1, beta 2, gamma).

The second ANOVA design compared the spatial distribution of resting state EEG sources in the mild AD group over time, using the regional LORETA solutions as a dependent variable. The ANOVA factors were Condition (Recording I, Recording II, dependent variable), Band (delta, theta, alpha 1, alpha 2, beta 1, beta 2, gamma), and ROI (central, frontal, parietal, occipital, temporal).

RESULTS

Demographic data

Table 2 summarizes the relevant demographic and clinical data of the recruited Nold and mild AD patients. *T*-testing for independent populations was computed to evaluate the presence or absence of statistically significant differences between the two groups (i.e., Nold and mild AD) for age, education, and MMSE ($p < 0.05$). Furthermore, Fisher exact test was computed to evaluate the presence or absence of statistically significant differences between the two groups for gender ($p < 0.05$). As expected, a statistically significant difference was found for MMSE ($p < 0.00001$; higher MMSE for Nold than mild AD subjects). On the contrary, no statistically significant difference was found for age, gender, and education ($p > 0.1$). However, the age, gender, and education values were used as covariates in the subsequent statistical analysis, to exclude that the small differences in age, gender, and education could influence the subsequent statistical analysis.

Topography of the EEG cortical sources as estimated by LORETA

For illustrative purpose, Fig. 2 maps the grand average of the LORETA solutions (i.e., relative power current density at cortical voxels) modeling the distributed EEG cortical sources for delta, theta, alpha 1, alpha 2, beta 1, beta 2, and gamma bands in the Nold and in the mild AD groups (Recording I). The Nold group presented alpha 1 sources with the maximal values of power distributed in the posterior regions. Delta, theta, and alpha 2 sources had moderate power values when compared to the alpha 1 sources. Finally, the beta 1, beta 2, and gamma sources were characterized by lowest power values. Compared to the Nold group, the mild AD group showed a strong power reduction of posterior alpha sources, along with a power increase of widespread delta sources.

Figure 3 maps the grand average of LORETA solutions (i.e., relative power current density at cortical voxels) modeling the distributed EEG sources for delta, theta, alpha 1, alpha 2, beta 1, beta 2, and gamma bands in the mild AD group at Recordings I and II. Compared to the Recordings I, the Recordings II was characterized by a decrease of widespread alpha and posterior beta 1 sources as well as an increase of widespread delta sources.

Statistical analysis of the LORETA solutions

The ANOVA for the evaluation of the control hypothesis (i.e., cortical sources of resting state EEG rhythms are different between Nold and AD subjects)

Table 2
Demographic and clinical data of the recruited normal elderly controls (Nold) and mild Alzheimer's disease subjects (mild AD)

	mild AD	Nold	*p*-value
n	88	35	
Age (years)	76.4 (±0.8 SE, from 58 to 90)	73.4 (±1.2 SE, from 62 to 91)	>0.2
Education (years)	5.7 (±0.3 SE, from 1 to 18)	8.3 (±0.8 SE, from 2 to 18)	>0.25
Gender (M/F)	19/69	6/29	>0.1
MMSE I	21.7 (±0.2 SE, from 17.2 to 25)	28.1 (±0.2 SE, from 25.7 to 30)	<0.00001
MMSE II	20 (±0.4 SE, from 10.7 to 25)	–	–

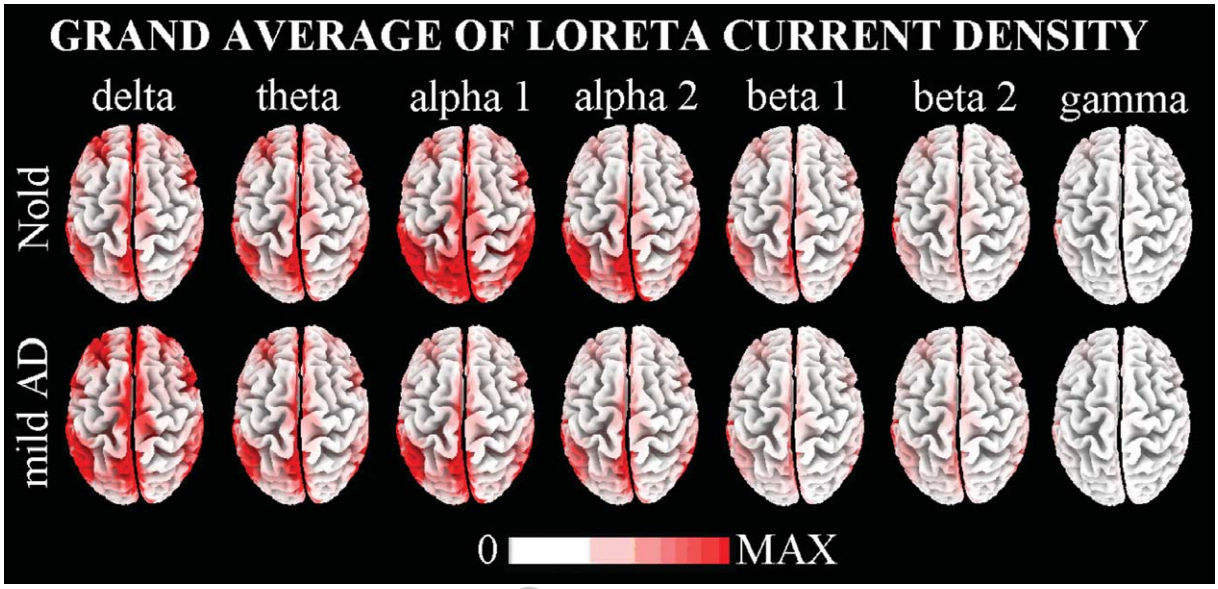

Fig. 2. Grand average of LORETA solutions (i.e., normalized relative current density at the cortical voxels) modeling the distributed EEG sources for delta, theta, alpha 1, alpha 2, beta 1, beta 2, and gamma bands in Nold, and mild AD (Recording I) groups. The left side of the maps (top view) corresponds to the left hemisphere. Legend: LORETA, low resolution brain electromagnetic tomography. Color scale: all power density estimates were scaled based on the averaged maximum value (i.e., alpha 1 power value of occipital region in Nold).

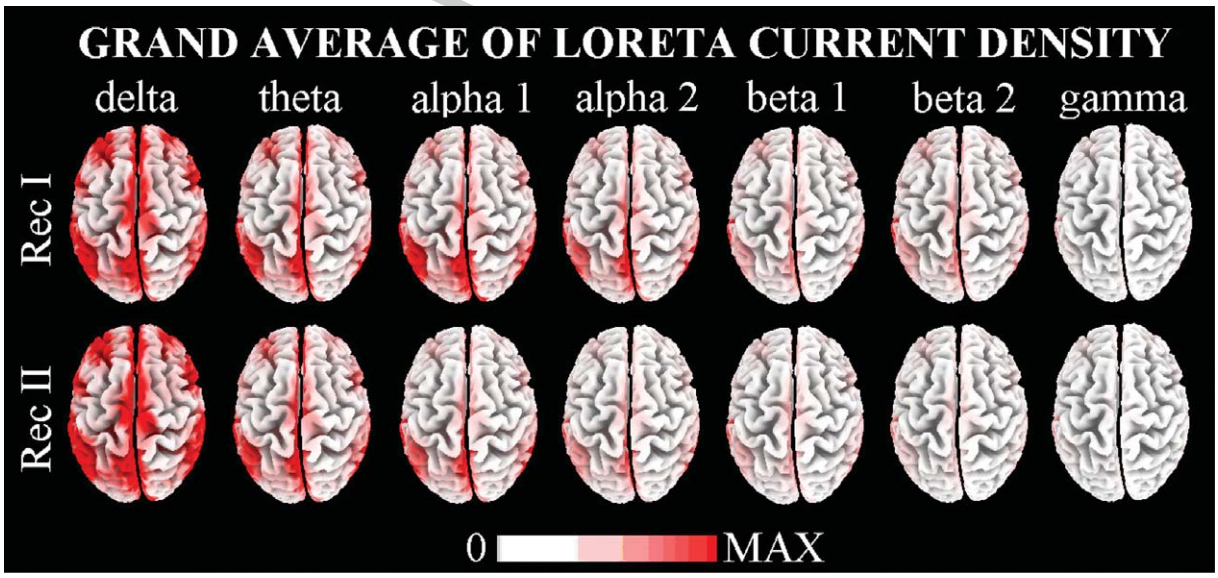

Fig. 3. Grand average of LORETA solutions (i.e., normalized relative current density at the cortical voxels) modeling the distributed EEG sources for delta, theta, alpha 1, alpha 2, beta 1, beta 2, and gamma bands in mild AD patients during Recording I and Recording II. The left side of the maps (top view) corresponds to the left hemisphere. Legend: LORETA, low resolution brain electromagnetic tomography. Color scale: all power density estimates were scaled based on the averaged maximum value.

showed a statistically significant interaction effect (df Effect = 24; MS Effect = 2.36; df Error = 2904; MS Error = 0.36; $F = 6.26$; $p < 0.0001$) among the factors Group (Nold, mild AD), Band (delta, theta, alpha 1, alpha 2, beta 1, beta 2, gamma), and ROI (frontal, central, parietal, occipital, temporal). Figure 4 reports the mean regional normalized LORETA solutions relative to this statistical interaction effect. The LORETA

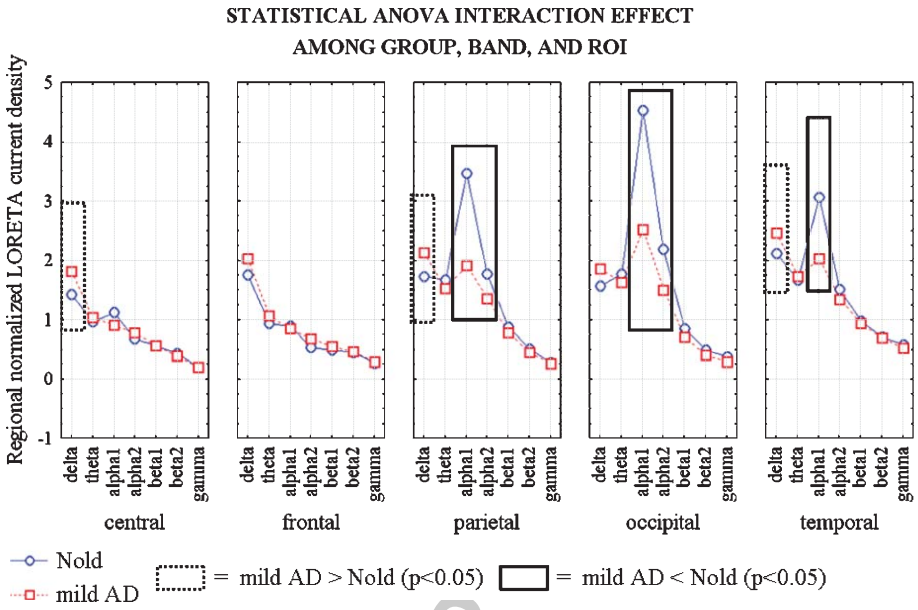

Fig. 4. Statistical ANOVA interaction effect (df Effect = 24; MS Effect = 2.36; df Error = 2904; MS Error = 0.36; $F = 6.26$; $p < 0.0001$) among the factors Group (Nold, mild AD), Band (delta, theta, alpha 1, alpha 2, beta 1, beta 2, gamma), and ROI (frontal, central, parietal, occipital, temporal). Legend: rectangles indicate the cortical regions and frequency bands in which LORETA solutions presented statistically different values ($p < 0.05$, Duncan *post-hoc* test) in Nold with respect to AD subjects.

solutions had the shape of EEG relative power spectra. Notably, the profile and power of these spectra in the Nold and in the mild AD group differed across various cortical macro-regions, thus supporting the idea that scalp EEG rhythms are generated by a distributed pattern of cortical sources. Planned *post-hoc* testing disclosed the pattern Nold > AD for the central, parietal, occipital, and temporal alpha 1 sources ($p < 0.000005$), as well as for the parietal and occipital alpha 2 sources ($p < 0.005$). Furthermore, the central, parietal, and temporal delta sources were lower in power in the Nold than in the AD group ($p < 0.01$). Table 3 reports p values (Duncan *post hoc*) and effect sizes (Cohen's d) [32] for the aforementioned cortical regions and frequency bands in which LORETA solutions presented statistically different values in Nold respect to mild AD ($p < 0.05$). These results were in line with previous EEG evidence of our group showing remarkable abnormalities of the cortical sources of the resting state delta and alpha rhythms in AD patients compared to Nold subjects [38–40, 41, 55–71, 73, 107]. Compared to the previous studies, the present investigation further demonstrated additional abnormalities of the posterior high-frequency alpha sources in the AD patients, possibly due to increasing the statistical power by analysis of a high number of enrolled AD patients.

Table 3
p values (Duncan *post hoc*), effect sizes (Cohen's d), and sample size (required to yield $p < 0.05$) for the cortical regions and frequency bands in which LORETA solutions presented statistically different values in Nold respect to mild AD ($p < 0.05$)

LORETA current density	p values	Effect sizes (Cohen's d)
Central delta	0.007	–0.37
Parietal delta	0.005	–0.31
Temporal delta	0.009	–0.3
Parietal alpha 1	0.000001	0.77
Occipital alpha 1	0.000003	0.63
Temporal alpha 1	0.000005	0.64
Parietal alpha 2	0.003	0.39
Occipital alpha 2	0.000002	0.46

The ANOVA for the evaluation of the working hypothesis (i.e., delta and alpha sources deteriorate along the progression of the disease) showed a statistically significant interaction effect (df Effect = 24; MS Effect = 0.56; df Error = 2088; MS Error = 0.14; $F = 3.93$; $p < 0.0001$) among the factors Condition (Recording I, Recording II), Band (delta, theta, alpha 1, alpha 2, beta 1, beta 2, gamma), and ROI (central, frontal, parietal, occipital, temporal). Figure 5 shows the mean regional normalized LORETA solutions relative to this statistical ANOVA interaction effect. The Duncan planned *post-hoc* testing showed that compared to Recording I, Recording II was characterized

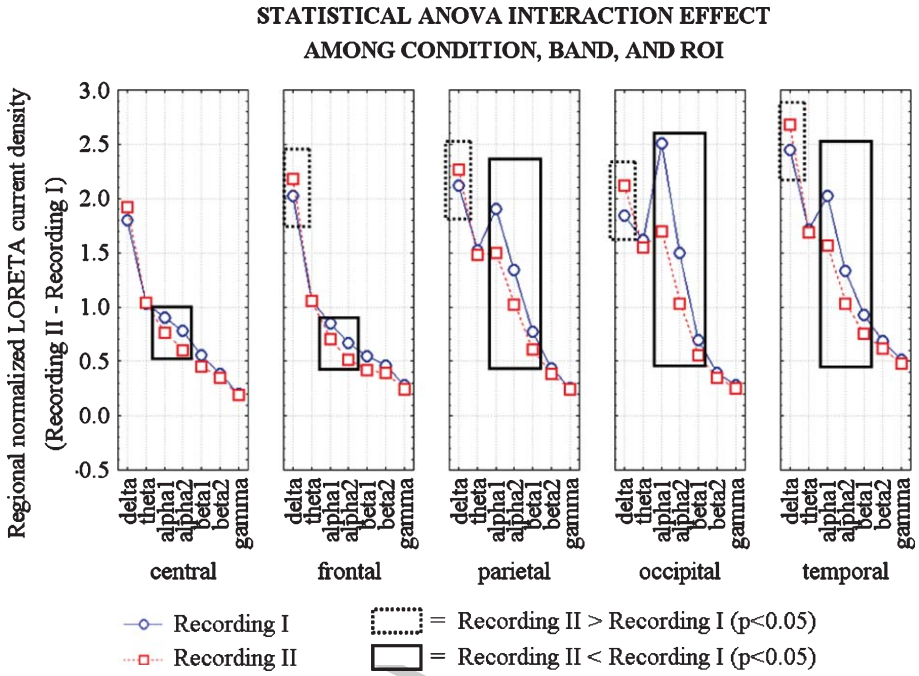

Fig. 5. Statistical ANOVA interaction effect df Effect = 24; MS Effect = 0.56; df Error = 2088; MS Error = 0.14; $F = 3.93$; $p < 0.0001$) among the factors Condition (Recording I, Recording II), Band (delta, theta, alpha 1, alpha 2, beta 1, beta 2, gamma), and ROI (frontal, central, parietal, occipital, temporal). Legend: rectangles indicate the cortical regions and frequency bands in which LORETA solutions presented statistically different values ($p < 0.05$, Duncan *post-hoc* test) in Recording I with respect to Recording II.

by lower power of the frontal, central, parietal, occipital, and temporal alpha 1 ($p < 0.05$) and alpha 2 ($p < 0.05$) sources. The same was true for the parietal, occipital, and temporal beta 1 sources ($p < 0.05$). In addition, the power of the frontal, parietal, occipital, and temporal delta sources ($p < 0.05$) was greater in the Recording II than in the Recording I. Table 4 reports *p* values (Duncan *post hoc*) and effect sizes (Cohen's d) for the cortical regions and frequency bands in which LORETA solutions presented statistically different values in Recording I with respect to Recording II ($p < 0.05$)

Table 4
p values (Duncan *post hoc*), effect sizes (Cohen's d), and sample size (required to yield $p < 0.05$) for the cortical regions and frequency bands in which LORETA solutions presented statistically different values ($p < 0.05$) in Recording II respect to Recording I

LORETA current density	*p* values	Effect sizes (Cohen's d)
Frontal delta	0.02	0.14
Parietal delta	0.02	0.11
Occipital delta	0.000007	0.23
Temporal delta	0.00007	0.19
Central alpha 1	0.02	–0.29
Frontal alpha 1	0.02	–0.37
Parietal alpha 1	0.000002	–0.29
Occipital alpha 1	0.000002	–0.42
Temporal alpha 1	0.000001	–0.38
Central alpha 2	0.008	–0.34
Frontal alpha 2	0.02	–0.45
Parietal alpha 2	0.000001	–0.34
Occipital alpha 2	0.000001	–0.43
Temporal alpha 2	0.000005	–0.42
Parietal beta 1	0.01	–0.37
Occipital beta 1	0.03	0.33
Temporal beta 1	0.008	–0.37

Additional analyses

To cross-validate the LORETA results reported above on the comparison between Recording II and Recording I in mild AD subjects, the analysis was directly repeated on the recorded EEG data used as input for the LORETA analyses. This was done to control for a possible effect of the source and head modeling procedures of the LORETA technique. The same frequency bands of interest of the LORETA analyses were considered, namely delta (2–4 Hz), theta (4–8 Hz), alpha 1 (8–10.5 Hz), alpha 2 (10.5–13 Hz), beta 1 (13–20 Hz), beta 2 (20–30 Hz), and gamma (30–40 Hz). Analogous to the LORETA analysis, five ROIs were considered. These ROIs included respectively: (i) C3, Cz, and C4 electrodes for the central region, (ii) F3, Fz, and F4 electrodes for the

frontal region, (iii) P3, Pz, and P4 electrodes for the parietal region, (iv) O1 and O2 electrodes for the occipital region, and (v) T3, T4, T5, and T6 for the temporal region. The same kind of normalization of the LORETA solutions was used for the EEG spectral solutions of this additional analysis. The spectral power density at each electrode was normalized to the spectral power density averaged across all frequencies (0.5–45 Hz) and across all electrodes. The values of the normalized spectral power density of the electrodes belonging to the same ROI were averaged at each of the seven frequency bands of interest. The results of this additional data analysis were used as inputs for an ANOVA. The values of the regional normalized spectral power density served as dependent variables. The ANOVA factors were Condition (Recording I, Recording II, dependent variable), Band (delta, theta, alpha 1, alpha 2, beta 1, beta 2, gamma), and ROI (central, frontal, parietal, occipital, temporal). Subjects' age, education, gender, and IAF peak were used as covariates. This ANOVA showed a statistically significant interaction effect (df Effect = 6; MS Effect = 8.19; df Error = 522; MS Error = 1.6; $F = 5.1$; $p < 0.0001$) between the factors Condition and Band. Figure 6 shows the mean normalized spectral power density relative to this statistical ANOVA interaction effect. The Duncan planned *post-hoc* testing showed that compared to Recording I, Recording II was characterized by lower alpha 1 ($p < 0.00005$) and alpha 2 power ($p < 0.001$), regardless of the factor ROI. In addition, the delta power was greater in Recording II than in the Recording I ($p < 0.05$). The present results confirmed, with less spatial resolution, those obtained by LORETA analysis. In particular, the absence of difference at beta band between Recording I and Recording II was predicted due to less spatial resolution of scalp EEG data.

As a further additional analysis, the LORETA source solutions of Recording I were correlated with MMSE score across all Nold and mild AD patients as single group (Pearson test, $p < 0.05$). The LORETA source solutions were those showing statistically significant *post-hoc* differences between the Nold and the mild AD group ($p < 0.05$). Results showed that the pathological delta sources negatively correlated to the MMSE score, whereas the correlation was positive between the alpha 1 and alpha 2 sources and the MMSE score. The significant correlations were observed with the parietal delta sources ($p < 0.05$), as well as with the parietal, occipital, and temporal alpha 1 and occipital alpha 2 sources ($p < 0.05$). Table 5 reports the r and p values of the statistically significant correlations between the LORETA source solutions of Recording I and the MMSE score ($p < 0.05$).

As another control analysis, we performed an ANOVA design to confirm the predicted decline of the MMSE score in the whole AD group at 1-year follow up. As expected, the analysis showed a statistically significant higher value of the MMSE score at baseline (i.e., MMSE I) compared to that recorded at the 1-year follow up (i.e., MMSE II; $p < 0.0001$). Afterwards, the power of the baseline (Recording I) delta and alpha 1

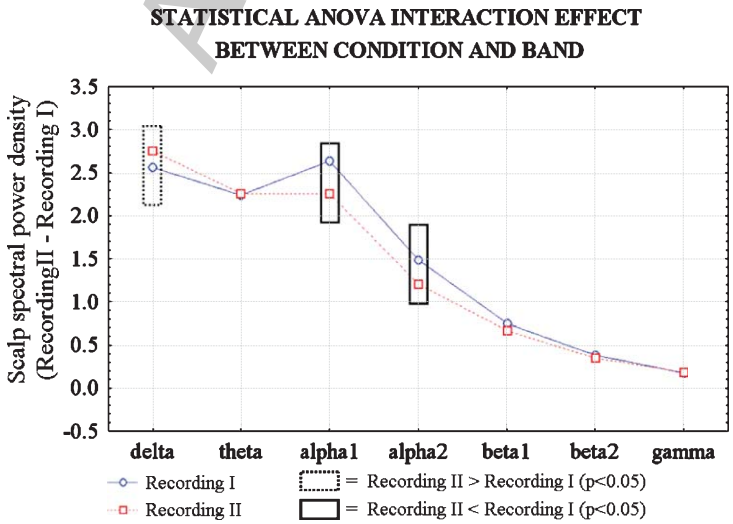

Fig. 6. Statistical ANOVA interaction (F(20,1740) = 4.15; $p < .00001$) between the factors Condition (Recording I, Recording II) and Band (delta, theta, alpha 1, alpha 2, beta 1, beta 2). Legend: rectangles indicate the cortical regions and frequency bands in which scalp spectral power density presented statistically different values ($p < 0.05$, Duncan *post-hoc* test) in Recording I with respect to Recording II.

Table 5
The r and p values of all statistically significant correlations between the LORETA source solutions of the Recording I and the MMSE score across the Nold and mild AD subjects as a single group ($p < 0.05$). The LORETA source solutions were those showing statistically significant *post-hoc* differences between the Nold and the mild AD group ($p < 0.05$)

Correlation between LORETA current density and MMSE score (r, p-value)	
Parietal delta LORETA versus MMSE	$r = –0.18$, $p = 0.05$
Parietal alpha 1 LORETA versus MMSE	$r = 0.22$, $p = 0.01$
Occipital alpha 1 LORETA versus MMSE	$r = 0.21$, $p = 0.02$
Temporal alpha 1 LORETA versus MMSE	$r = 0.22$, $p = 0.01$
Occipital alpha 2 LORETA versus MMSE	$r = 0.19$, $p = 0.03$

sources showing remarkable differences between the Nold and the AD group was used as an input for an exploratory statistical correlation with the difference of the MMSE score between baseline and 1-year follow-up (MMSE II – MMSE I) in the mild AD patients (Pearson test, $p < 0.05$). Figure 7 shows that there was a statistically significant negative correlation between the temporal delta sources and the MMSE score difference (MMSE II – MMSE I; $r = –0.21$, $p = 0.04$). The higher the power of the temporal delta sources at the baseline recording, the lower was the decline of the global cognition as measured by the MMSE at 1-year follow up (MMSE II –MMSE I).

A further additional analysis was performed to ensure that the above described LORETA source differences between Recording II and Recording I in mild AD were not due to the large number of subjects used for the analysis. To address this issue, we considered a sub-group of mild AD subjects ($n = 40$; 10 female; mean age: 76.8 ± 1 SE; mean education: 5.2 ± 0.4 SE). An ANOVA using the regional LORETA solutions as a dependent variable and the factors Condition (Recording I, Recording II), Band (delta, theta, alpha 1, alpha 2, beta 1, beta 2, gamma), and ROI (central, frontal, parietal, occipital, temporal) was performed. The ANOVA showed a statistically significant interaction effect (df Effect = 24; MS Effect = 0.3; df Error = 936; MS Error = 0.11; $F = 2.63$; $p < 0.0001$). Figure 8 shows the mean regional normalized LORETA solutions relative to this statistical ANOVA interaction effect. The Duncan planned *post-hoc* testing showed that compared to Recording I, Recording II was characterized by lower power of the parietal, occipital, and temporal alpha 1 ($p < 0.000005$) as well as central, parietal, occipital, and temporal alpha 2 ($p < 0.05$) sources. The same was true for the parietal, occipital, and temporal beta 1 sources ($p < 0.05$). In addition, the power of the central, frontal, parietal, occipital, and temporal delta sources ($p < 0.005$) was greater in Recording II compared to Recording I. This control ANOVA analysis globally confirmed the results obtained with the whole group.

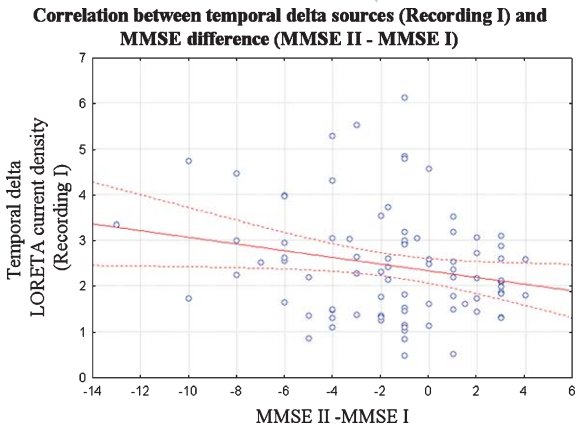

Fig. 7. Scatterplots of LORETA solutions for the temporal delta sources and the difference of MMSE values (MMSE II –MMSE I) in the mild AD patients. Statistical values of linear correlation ($r = –0.21$, $p = 0.04$) were obtained by Pearson test ($p < 0.05$).

The comparison between the results obtained with $n = 40$ and $n = 88$ mild AD subjects highlights a crucial question on the sample size of mild AD subjects that must be used to study disease state or progression in clinical trials. The sample size used in a study is determined based on the previous data collection, and to ensure sufficient statistical power. Here, we evaluated the sample size required to yield a statistical power of $p < 0.05$ using the EEG results obtained with 88 mild AD subjects and 35 Nold subjects. We decided to use EEG results on posterior alpha 1 sources that presented a higher difference either in the comparison between Nold and mild AD subjects (disease state markers) or in the comparison between Recording I and Recording II in mild AD patients (disease progression markers). Sample size was calculated using Cohen's tables [32]. Table 6 reports the sample sizes required to yield a statistical power $p < 0.05$ using EEG data of parietal, occipital and temporal alpha 1 sources. The results suggests the minimum sample size to study disease state with the EEG markers was about 30 subjects, whereas the minimum sample size to study disease progression was about 100 subjects.

As a last additional analysis, we evaluated the variance of the LORETA solutions in the mild AD subjects. To address this issue, we measured the coefficient of variation (CV) for the difference of regional normalized LORETA solutions between Recording II and Recording I. Table 7 reports the CV values for the seven bands (delta, theta, alpha 1, alpha 2, beta 1,

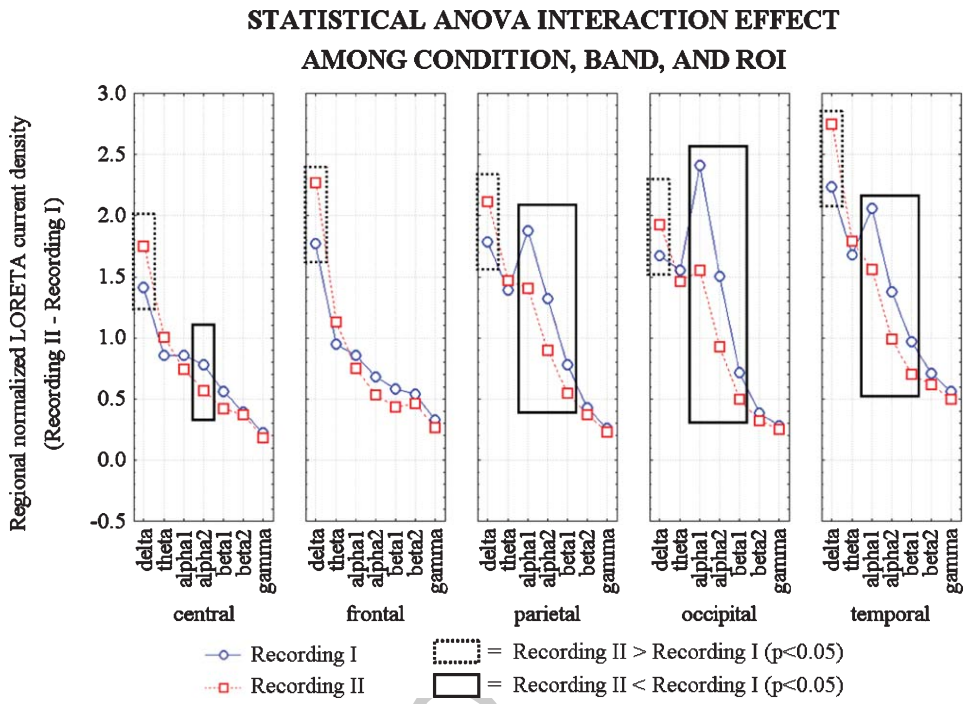

Fig. 8. Statistical ANOVA interaction effect (df Effect = 24; MS Effect = 0.3; df Error = 936; MS Error = 0.11; $F = 2.63$; $p < 0.0001$) among the factors Condition (Recording I, Recording II), Band (delta, theta, alpha 1, alpha 2, beta 1, beta 2), and ROI (frontal, central, parietal, occipital, temporal). Legend: rectangles indicate the cortical regions and frequency bands in which LORETA solutions presented statistically different values ($p < 0.05$, Duncan *post-hoc* test) in Recording I with respect to Recording II.

Table 6
Sample sizes required to yield a statistical power $p < 0.05$ using EEG data of parietal, occipital and temporal alpha 1 sources of mild AD ($n = 88$) and Nold ($n = 35$) subjects. Sample size was calculated using Cohen's tables

Sample size required to yield $p < 0.05$		
	AD disease state (Nold versus mild AD)	AD progression
Parietal alpha 1	22	148
Occipital alpha 1	32	71
Temporal alpha 1	31	87

Table 7
Values of coefficient of variation (CV) for the difference of regional normalized LORETA solutions between Recording II and Recording I in mild AD groups. The CV values are reported for seven Band (delta, theta, alpha 1, alpha 2, beta 1, beta 2, gamma) and five ROI (frontal, central, parietal, occipital, temporal)

Coefficient of variation (CV)					
	Central	Frontal	Parietal	Occipital	Temporal
Delta	0.09	0.12	0.1	0.21	0.16
Theta	0.02	0.01	0.04	0.05	0.04
Alpha 1	0.28	0.34	0.29	0.37	0.39
Alpha 2	0.4	0.4	0.33	0.39	0.40
Beta 1	0.36	0.45	0.39	0.37	0.39
Beta 2	0.09	0.14	0.18	0.11	0.14
Gamma	0.19	0.22	0.22	0.32	0.36

beta 2, gamma) and five ROIs (frontal, central, parietal, occipital, temporal). The CV values were lower than 0.45 suggesting that the distribution of LORETA solutions in the mild AD subjects can be considered at low-variance (this is typically the case of CV <1; CV <1 would denote high variance).

Finally, to evaluate the absence of remarkable outlier, Figure 9 illustrates the individual values of the difference of regional normalized LORETA solutions between Recording II and Recording I. In particular, the difference of regional normalized LORETA solutions are represented for seven band (delta, theta, alpha 1, alpha 2, beta 1, beta 2, gamma) and five ROI (frontal, central, parietal, occipital, temporal). The figure shows the absence of remarkable outliers.

Table 8 summarizes the results of all above mentioned statistical results.

DISCUSSION

We tested the hypothesis that the cortical sources of resting state EEG rhythms were sensitive to both

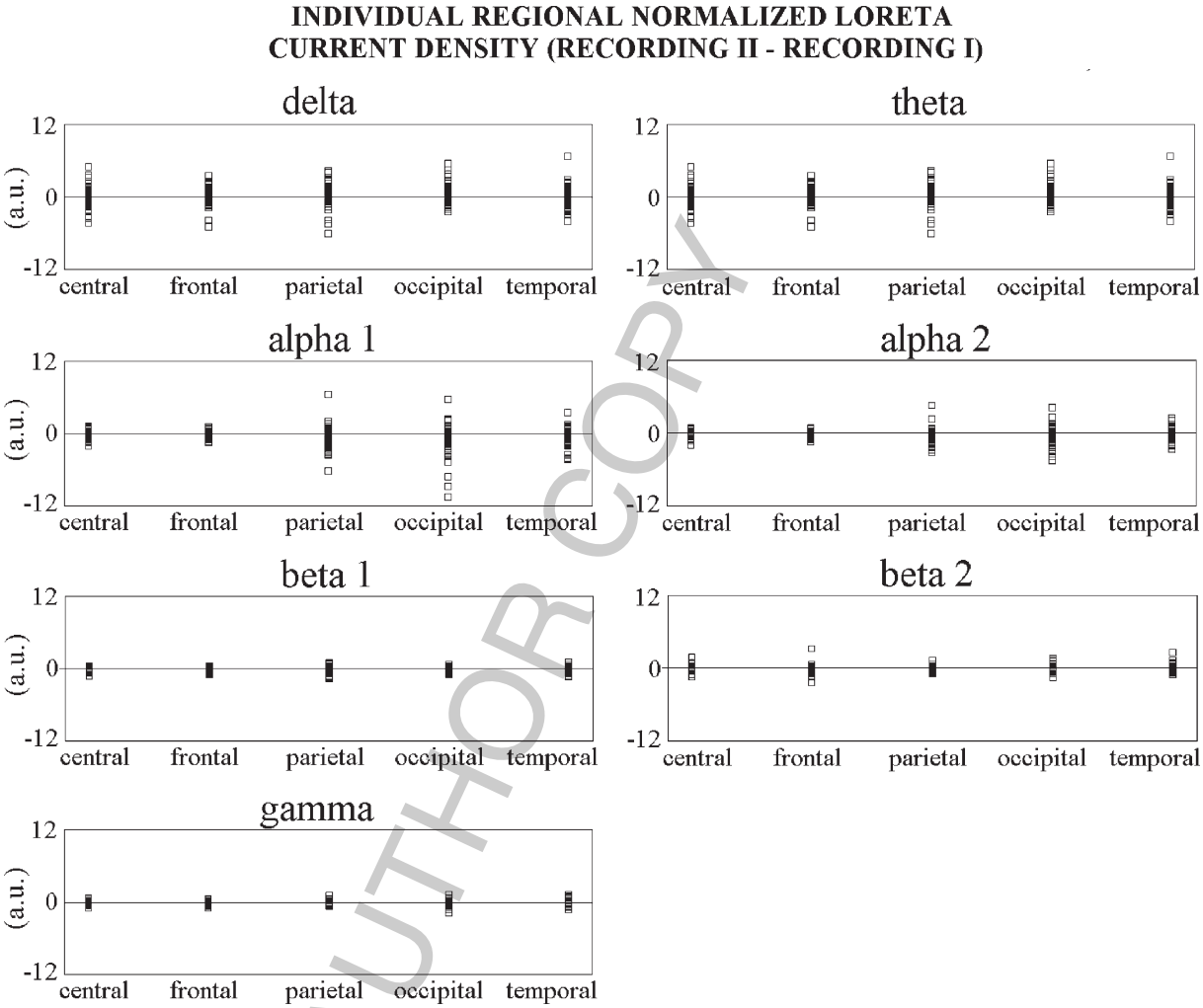

Fig. 9. Individual values of the difference of regional normalized LORETA solutions between Recording II and Recording I. In particular, the difference of regional normalized LORETA solutions are represented for the seven band (delta, theta, alpha 1, alpha 2, beta 1, beta 2, gamma), and five ROI (frontal, central, parietal, occipital, temporal).

disease state and progression in a large cohort of mild AD patients. The EEG source markers of the disease state were first extracted from the patients' baseline EEG recordings. The central, parietal, occipital, and temporal alpha sources at low-frequency as well as the parietal and occipital alpha sources at high-frequency were lower in power in the mild AD patients than in the Nold subjects. Furthermore, the central, parietal, and temporal delta sources were higher in power in the mild AD patients than in the Nold subjects. These results extend previous EEG data generated from our group showing remarkable abnormalities of the posterior cortical sources of the resting state delta and alpha rhythms in AD patients compared to Nold subjects [38–41, 55–71, 73, 107]. Compared to the previous studies, the present investigation demonstrated additional abnormalities of the posterior high-frequency alpha sources in the AD patients, possibly due to the optimal statistical power enabled by the large cohort of AD patients.

As a second step of the study, the EEG source markers of AD progression were obtained by a comparison between baseline and 1-year follow up EEG recordings. The central, frontal, parietal, occipital, and temporal alpha sources at low- and high-frequency were lower in power in the 1-year follow up than in the baseline EEG recordings, along with a slight decrease in power of parietal, occipital, and temporal beta sources at low-frequency. Furthermore, the frontal, parietal, occipital, and temporal delta sources

Table 8
Summary of the statistical results

Design	Statistical Comparisons	Results
To test possible differences between the Nold and mild AD for age, education, gender, MMSE	*T*-test (age, education, MMSE) Fisher exact test (gender)	No statistically significant difference between the Nold and mild AD for age, education, and gender ($p > 0.1$) Statistically significant difference for MMSE value $p < 0.00001$): MMSE was lower in the mild AD than Nold
To test possible difference in the individual alpha frequency peak (IAF peak) between the Nold and mild AD	*T*-test	Statistically significant difference ($p < 0.05$): IAF was lower in the mild AD than Nold
To test possible difference in the IAF peak between Recording I and Recording II in the mild AD	*T*-test	Statistically significant difference ($p < 0.05$): IAF peak was lower at Recording II than Recording I in the mild AD
To compare cortical (LORETA) sources of EEG rhythms between the Nold and mild AD at Recording I	ANOVA *Factors:* Group (Nold, mild AD), Band (delta, theta, alpha1, alpha2, beta1, beta2, gamma), ROI (central, frontal, parietal, occipital, temporal) *Covariates:* Age, gender, education, IAF	Statistically significant interaction effect among the factors Group, Band, and ROI ($F = 6.3$; $p < 0.0001$). Duncan planned *post-hoc* testing disclosed: (i) the pattern Nold > AD for parietal, occipital and temporal alpha 1 sources ($p < 0.000005$) as well as for parietal and occipital alpha 2 sources ($p < 0.005$); (ii) the pattern Nold < AD for central, parietal, and temporal delta sources ($p < 0.01$)
To compare cortical (LORETA) sources of EEG rhythms between Recording I and Recording II in mild AD	ANOVA *Factors:* Condition (Recording I, Recording II), Band (delta, theta, alpha1, alpha2, beta1, beta2, gamma), ROI (central, frontal, parietal, occipital, temporal)	Statistically significant interaction effect among the factors Condition, Band, and ROI ($F = 3.9$; $p < 0.0001$). Duncan planned *post-hoc* testing disclosed: (i) the pattern Recording II< Recording I for frontal, central, parietal, occipital, and temporal alpha 1 and alpha 2 ($p < 0.05$) sources as well as for parietal, occipital, and temporal beta 1 ($p < 0.05$); (ii) the pattern Recording II > Recording I for frontal, parietal, occipital, and temporal delta sources ($p < 0.05$)
To compare scalp EEG rhythms between Recording I and Recording II in mild AD	ANOVA *Factors:* Condition (Recording I, Recording II), Band (delta, theta, alpha1, alpha2, beta1, beta2), ROI (central, frontal, parietal, occipital, temporal)	Statistically significant interaction effect between the factors Condition and Band ($F = 5.1$; $p < 0.0001$). Duncan planned *post-hoc* testing disclosed: (i) the pattern Recording II < Recording I for alpha 1 ($p < 0.00005$) and alpha 2 sources ($p < 0.001$); (ii) the pattern Recording II > Recording I for delta sources ($p < 0.05$)
To test the correlation between LORETA source solutions of the Recording I and MMSE across Nold and mild AD	Pearson test	Statistically significant correlations between MMSE score and parietal delta sources ($p < 0.05$), as well as with the parietal, occipital, and temporal alpha 1 and occipital alpha 2 sources ($p < 0.05$)
To evaluate the expected decline of the MMSE score in the mild AD at 1-year follow up	*T*-test	Statistically significant difference ($p < 0.0001$): MMSE was lower at Recording II than Recording I in the mild AD
To evaluate the correlation between LORETA source solutions of the Recording I and difference of the MMSE score between baseline and 1-year follow-up (MMSE II – MMSE I) in mild AD	Pearson test	Statistically significant negative correlation between temporal delta sources and MMSE difference ($p < 0.05$)
To compare cortical (LORETA) sources of EEG rhythms between Recording I and Recording II in a sub-group of mild AD	ANOVA *Factors:* Condition (Recording I, Recording II), Band (delta, theta, alpha1, alpha2, beta1, beta2, gamma), ROI (central, frontal, parietal, occipital, temporal)	Statistically significant interaction effect among the factors Condition, Band, and ROI ($F = 2.63$; $p < 0.0001$). Duncan planned *post-hoc* testing disclosed: (i) the pattern Recording II < Recording I for parietal, occipital, and temporal alpha 1, for central, parietal, occipital, and temporal alpha 2, for parietal, occipital, and temporal beta 1 sources ($p < 0.05$); (ii) the pattern Recording II > Recording I for central, frontal, parietal, occipital, and temporal delta sources ($p < 0.05$)

were higher in power in the 1-year follow up compared to baseline EEG recordings. These results provide further evidence, extended to the spatial source domain, to add to longitudinal EEG studies showing that at about 2-years follow up, MCI patients were characterized by a power increase of delta and theta rhythms in temporal and occipital scalp regions associated to a power reduction of beta rhythms [51]. Furthermore, AD patients presented a power increase of delta and theta rhythms in temporal, parietal and/or occipital scalp regions when tested at 1–3 years follow up [49, 50].

The present study differs from previous studies in that the EEG source markers of the disease state and progression are computed and compared in our large cohort of AD patients. Common EEG source markers of the disease state and progression were observed at central, parietal, and temporal delta rhythms, at central, parietal, occipital, and temporal low-frequency alpha rhythms, and at parietal and occipital high-frequency alpha rhythms. Particular EEG source markers of the disease progression were observed at parietal, occipital, and temporal low-frequency beta rhythms. A hypothesis of the neurophysiological mechanism of the present results is proposed on the basis of the following theoretical considerations. In the condition of slow-wave sleep, corticofugal slow oscillations (<1 Hz) are effective in grouping thalamic-generated delta rhythms (1–4 Hz) and spindling activity (7–14 Hz) rhythms [108]. During wake up, spindles as well as high and low components of the delta rhythms are blocked by the inhibition of oscillators within, respectively, reticulo-thalamic (7–14 Hz), thalamo-cortical (1–4 Hz), and intracortical (<1 Hz), neuronal circuits [108]. In awake subjects, delta rhythms are considered a sign of brain damage, namely of disconnection of the cortico-cortical wiring [109, 110]. In the condition of awake resting state eyes-closed condition, dominant low-frequency alpha rhythms (about 8–10 Hz) would denote the synchronization of diffuse neural networks regulating the fluctuation of a subject's global arousal and consciousness states, whereas high-frequency alpha rhythms (about 10–12 Hz) would denote the synchronization of more selective neural networks specialized in the processing of modal specific or semantic information [36, 111]. When the subject is engaged in sensorimotor or cognitive tasks, alpha and low-frequency beta rhythms reduce in amplitude (i.e., "de-synchronization or blocking") and are replaced by fast EEG oscillations at high-frequency beta (about 20–30 Hz) and gamma (>30 Hz) rhythms [111]. An unresolved issue is the complex interaction of ascending neurotransmitter systems for the regulation of the resting state EEG rhythms (i.e., glutamergic, cholinergic, serotoninergic, istaminergic, noradrenergic, GABAergic, etc.). In this complex interaction, alpha rhythms might mainly depend on cholinergic, glutamatergic, and GABAergic neuromodulatory systems as demonstrated in recent animal studies on populations of thalamic and cortical neurons [112, 113].

Keeping in mind these data and theoretical considerations, it can be speculated that in the resting state eyes-closed condition, the EEG source markers of the AD state and disease progression would reflect an abnormal enhancement of the pathological EEG slow-frequency rhythms (i.e., delta and theta) as a cortical "disconnection mode" impinging upon thalamo-cortical circuits [108–116]. Furthermore, there might be an abnormal tonic desynchronization of the cortical alpha rhythms indicating an exaggerated and unselective activation of brain networks underlying vigilance (i.e., arousal) and semantic/sensorimotor functions [36, 111]. In addition, the EEG source markers of AD progression would reflect a worsening of the above pathological mechanisms in terms of magnitude and enhancing effects on higher EEG frequencies (i.e., beta).

CONCLUSIONS

Previous evidence has shown that cortical sources of resting state EEG rhythms are abnormal in subjects with AD. Here we tested the hypothesis that these sources were also sensitive to the progression of AD over 1 year. To this aim, the resting state eyes-closed EEG data were recorded in a large cohort of mild AD patients and in control Nold subjects. Along the observation period of about 1 year, the mild AD patients lost about 2 points of MMSE score, on average. Compared to the Nold subjects, the mild AD patients were characterized by a power increase of widespread delta sources and by a power decrease of posterior alpha sources (i.e., EEG markers of "disease state"). In the mild AD patients, the 1-year follow-up EEG recordings showed increased power of widespread delta sources as well as decreased power of widespread alpha and posterior beta 1 sources (i.e., EEG markers of "disease progression"). These results suggest that the resting state EEG sources seem to be sensitive, at least at group level, to the cognitive decline that occurred in the mild AD group over 1 year, and might represent cost-effective, non-invasive, and popular markers to follow the disease tracking of large AD populations in clinical trials.

A future crucial issue will be to evaluate whether resting state EEG sources can measure cognitive decline (i.e., disease progression) in a single AD subject. Future study using artificial neural networks or other mathematical predictors (i.e., Bayesian) will address this interesting point.

ACKNOWLEDGMENTS

We thank Prof./Drs. Katarzyna Blinowska, Franciszek Rakowski, Fabrizio Vecchio, and Maciej Kaminski for their fruitful comment and advice on this study. This research was developed thank to the financial support by the Italian Ministry of Health, GR-2008-1143091 and GR-2008-1143090 projects., as well as by European Committee in the framework of the FP7-"ICT Infrastructure" project entitled "Diagnostic Enhancement of Confidence by an International Distributed Environment" ("DECIDE", Grant Agreement: RI-261593). Please find complete information about the DECIDE Consortium and principal investigators at http://www.decide-collaboration.eu/.

Authors' disclosures available online (http://www.j-alz.com/disclosures/view.php?id=1621).

REFERENCES

[1] Lanctot KL, Herrmann N, Kenneth KY, Khan LR, Liu BA, Loulou MM, Einarson TR (2003) Efficacy and safety of cholinesterase inhibitors in Alzheimer's disease: A meta-analysis. *CMAJ* **169**, 557-564.

[2] Dubois B, Feldman HH, Jacova C, Dekosky ST, Barberger-Gateau P, Cummings J, Delacourte A, Galasko D, Gauthier S, Jicha G, Meguro K, O'brien J, Pasquier F, Robert P, Rossor M, Salloway S, Stern Y, Visser PJ, Scheltens P. (2007) Research criteria for the diagnosis of Alzheimer's disease: Revising the NINCDS-ADRDA criteria. *Lancet Neurol* **6**, 734-746.

[3] Albert MS, DeKosky ST, Dickson D, Dubois B, Feldman HH, Fox NC, Gamst A, Holtzman DM, Jagust WJ, Petersen RC, Snyder PJ, Carrillo MC, Thies B, Phelps CH (2011) The diagnosis of mild cognitive impairment due to Alzheimer's disease: Recommendations from the National Institute on Aging-Alzheimer's Association workgroups on diagnostic guidelines for Alzheimer's disease. *Alzheimers Dement* **7**, 270-279.

[4] Jack CR Jr, Bernstein MA, Borowski BJ, Gunter JL, Fox NC, Thompson PM, Schuff N, Krueger G, Killiany RJ, Decarli CS, Dale AM, Carmichael OW, Tosun D, Weiner MW (2010) Alzheimer's Disease Neuroimaging Initiative. Update on the magnetic resonance imaging core of the Alzheimer's disease neuroimaging initiative. *Alzheimers Dement* **6**, 212-220.

[5] McKhann GM, Knopman DS, Chertkow H, Hyman BT, Jack CR Jr, Kawas CH, Klunk WE, Koroshetz WJ, Manly JJ, Mayeux R, Mohs RC, Morris JC, Rossor MN, Scheltens P, Carrillo MC, Thies B, Weintraub S, Phelps CH (2011) The diagnosis of dementia due to Alzheimer's disease: Recommendations from the National Institute on Aging-Alzheimer's Association workgroups on diagnostic guidelines for Alzheimer's disease. *Alzheimers Dement* **7**, 263-269.

[6] Sperling R (2011) Potential of functional MRI as a biomarker in early Alzheimer's disease. *Neurobiol Aging* **32**(Suppl 1), S37-S43.

[7] Tapiola T, Alafuzoff I, Herukka SK, Parkkinen L, Hartikainen P, Soininen H, Pirttilä T (2009) Cerebrospinal fluid {beta}-amyloid 42 and tau proteins as biomarkers of Alzheimer-type pathologic changes in the brain. *Arch Neurol* **66**, 382-389.

[8] Frisoni GB, Fox NC, Jack CR Jr, Scheltens P, Thompson PM (2010) The clinical use of structural MRI in Alzheimer disease. *Nat Rev Neurol* **6**, 67-77.

[9] Silbert LC, Quinn JF, Moore MM, Corbridge E, Ball MJ, Murdoch G, Sexton G, Kaye JA (2003) Changes in premorbid brain volume predict Alzheimer's disease pathology. *Neurology* **61**, 487-492.

[10] Zarow C, Vinters HV, Ellis WG, Weiner MW, Mungas D, White L, Chui HC (2005) Correlates of hippocampal neuron number in Alzheimer's disease and ischemic vascular dementia. *Ann Neurol* **57**, 896-903.

[11] Schuff N (2009) Potential role of high-field MRI for studies in Parkinson's disease. *Mov Disord* **24**(Suppl 2), S684-S690.

[12] van de Pol LA, Hensel A, Barkhof F, Gertz HJ, Scheltens P, van der Flier WM (2006) Hippocampal atrophy in Alzheimer disease: Age matters. *Neurology* **66**, 236-238.

[13] Jagust W, Reed B, Mungas D, Ellis W, Decarli C (2007) What does fluorodeoxyglucose PET imaging add to a clinical diagnosis of dementia? *Neurology* **69**, 871-877.

[14] Minoshima S, Shimizu N (1997) [Genome information database]. *Tanpakushitsu Kakusan Koso* **42**(17 Suppl), 3038-3045.

[15] Klunk WE, Engler H, Nordberg A, Wang Y, Blomqvist G, Holt DP, Bergström M, Savitcheva I, Huang GF, Estrada S, Ausén B, Debnath ML, Barletta J, Price JC, Sandell J, Lopresti BJ, Wall A, Koivisto P, Antoni G, Mathis CA, Långström B (2004) Imaging brain amyloid in Alzheimer's disease with Pittsburgh Compound-B. *Ann Neurol* **55**, 306-319.

[16] Rowe CC, Ng S, Ackermann U, Gong SJ, Pike K, Savage G, Cowie TF, Dickinson KL, Maruff P, Darby D, Smith C, Woodward M, Merory J, Tochon-Danguy H, O'Keefe G, Klunk WE, Mathis CA, Price JC, Masters CL, Villemagne VL (2007) Imaging beta-amyloid burden in aging and dementia. *Neurology* **68**, 1718-1725.

[17] Ikonomovic MD, Klunk WE, Abrahamson EE, Mathis CA, Price JC, Tsopelas ND, Lopresti BJ, Ziolko S, Bi W, Paljug WR, Debnath ML, Hope CE, Isanski BA, Hamilton RL, DeKosky ST (2008) Post-mortem correlates of *in vivo* PiB-PET amyloid imaging in a typical case of Alzheimer's disease. *Brain* **131**(Pt 6), 1630-1645.

[18] Claus JJ, Strijers RL, Jonkman EJ, Ongerboer de Visser BW, Jonker C, Walstra GJ, Scheltens P, van Gool WA (1999) The diagnostic value of electroencephalography in mild senile Alzheimer's disease. *Clin Neurophysiol* **110**, 825-832.

[19] Huang C, Wahlund L, Dierks T, Julin P, Winblad B, Jelic V (2000) Discrimination of Alzheimer's disease and mild cognitive impairment by equivalent EEG sources: A cross-sectional and longitudinal study. *Clin Neurophysiol* **111**, 1961-1967.

[20] Bennys K, Rondouin G, Vergnes C, Touchon J (2001) Diagnostic value of quantitative EEG in Alzheimer disease. *Neurophysiol Clin* **31**, 153-160.
[21] Lehmann C, Koenig T, Jelic V, Prichep L, John RE, Wahlund LO, Dodge Y, Dierks T (2007) Application and comparison of classification algorithms for recognition of Alzheimer's disease in electrical brain activity (EEG). *J Neurosci Methods* **161**, 342-350.
[22] Bonanni L, Thomas A, Tiraboschi P, Perfetti B, Varanese S, Onofrj M (2008) EEG comparisons in early Alzheimer's disease, dementia with Lewy bodies and Parkinson's disease with dementia patients with a 2-year follow-up. *Brain* **131**(Pt 3), 690-705.
[23] Ommundsen N, Engedal K, Øksengård AR (2011) Validity of the quantitative EEG statistical pattern recognition method in diagnosing Alzheimer's disease. *Dement Geriatr Cogn Disord* **31**, 195-201.
[24] Dierks T, Ihl R, Frolich L, Maurer K (1993) Dementia of the Alzheimer type: Effects on the spontaneous EEG described by dipole sources. *Psychiatry Res* **50**, 151-162.
[25] Dierks T, Jelic V, Pascual-Marqui RD, Wahlund LO, Julin P, Linden DEJ, Maurer K, Winblad B, Nordberg A (2000) Spatial pattern of cerebral glucose metabolism (PET) correlates with localization of intracerebral EEG-generators in Alzheimer's disease. *Clin Neurophysiol* **111**, 1817-1824.
[26] Ponomareva NV, Selesneva ND, Jarikov GA (2003) EEG alterations in subjects at high familial risk for Alzheimer's disease. *Neuropsychobiology* **48**, 152-159.
[27] Jeong J (2004) EEG dynamics in patients with Alzheimer's disease. *Clin Neurophysiol* **115**, 1490-1505.
[28] Wolf H, Jelic V, Gertz HJ, Nordberg A, Julin P, Wahlund LO (2003) A critical discussion of the role of neuroimaging in mild cognitive impairment. *Acta Neurol Scand Suppl* **179**, 52-76.
[29] Moretti DV, Babiloni C, Binetti G, Cassetta E, Dal Forno G, Ferreri F, Ferri R, Lanuzza Bartolo, Miniussi C, Nobili F, Rodriguez G, Salinari S, Rossini PM (2004) Individual analysis of EEG frequency and band power in mild Alzheimer's disease. *Clin Neurophysiol* **115**, 299-308.
[30] Adeli H, Ghosh-Dastidar S, Dadmehr (2005) Alzheimer's disease: Models of computation and analysis of EEGs. *Clin EEG Neurosci* **36**, 131-140.
[31] Prichep LS, John ER, Ferris SH, Reisberg B, Almas M, Alper K, Cancro R (1994) Quantitative EEG correlates of cognitive deterioration in the elderly. *Neurobiol Aging* **15**, 85-90.
[32] Koenig T, Prichep L, Dierks T, Hubl D, Wahlund LO, John ER, Jelic V (2005) Decreased EEG synchronization in Alzheimer's disease and mild cognitive impairment. *Neurobiol Aging* **26**, 165-171.
[33] van Deursen JA, Vuurman EF, Verhey FR, van Kranen-Mastenbroek VH, Riedel WJ (2008) Increased EEG gamma band activity in Alzheimer's disease and mild cognitive impairment. *J Neural Transm* **115**, 1301-1311.
[34] Jelic V, Blomberg M, Dierks T, Basun H, Shigeta M, Julin P, Jensen M, Lannfelt L, Winblad B, Wahlund LO (1998) EEG slowing and cerebrospinal fluid tau levels in patients with cognitive decline. *Neuroreport* **9**, 157-160.
[35] Rodriguez G, Nobili F, Rocca G, DeCarli F, Gianelli MV, Rosadini G (1998) Quantitative electroencephalography and regional cerebral blood flow: Discriminant analysis between Alzheimer's patients and healthy controls. *Dement Geriatr Cogn Disord* **9**, 238-274.
[36] Klimesch W (1999) EEG alpha and theta oscillations reflect cognitive and memory performance: A review and analysis. *Brain Res Rev* **29**, 169-195.
[37] Neubauer AC, Freudenthaler HH (1995) Ultradian rhythms in cognitive performance: No evidence for a 1.5-h rhythm. *Biol Psychol* **40**, 281-298.
[38] Babiloni C, Binetti G, Cassarino A, Dal Forno G, Del Percio C, Ferreri F, Ferri R, Frisoni G, Galderisi S, Hirata K, Lanuzza B, Miniussi C, Mucci A, Nobili F, Rodriguez G, Romani GL, Rossini PM (2006) Sources of cortical rhythms in adults during physiological aging: A multi-centric EEG study. *Human Brain Mapp* **27**, 162-172.
[39] Babiloni C, Cassetta E, Binetti G, Tombini M, Del Percio C, Ferreri F, Ferri R, Frisoni G, Lanuzza B, Nobili F, Parisi L, Rodriguez G, Frigerio L, Gurzì M, Prestia A, Vernieri F, Eusebi F, Rossini PM (2007) Resting EEG sources correlate with attentional span in mild cognitive impairment and Alzheimer's disease. *Eur J Neurosci* **25**, 3742-3757.
[40] Roh JH, Park MH, Ko D, Park KW, Lee DH, Han C, Jo SA, Yang KS, Jung KY (2011) Region and frequency specific changes of spectral power in Alzheimer's disease and mild cognitive impairment. *Clin Neurophysiol* **122**, 2169-2176.
[41] Babiloni C, Binetti G, Cassetta E, Dal Forno G, Del Percio C, Ferreri F, Ferri R, Frisoni G, Hirata K, Lanuzza B, Miniussi C, Moretti DV, Nobili F, Rodriguez G, Romani GL, Salinari S, Rossini PM (2006) Sources of cortical rhythms change as a function of cognitive impairment in pathological aging: A multi-centric study. *Clin Neurophysiol* **117**, 252-268.
[42] Farlow M, Anand R, Messina J Jr, Hartman R, Veach J (2000) A 52-week study of the efficacy of rivastigmine in patients with mild to moderately severe Alzheimer's disease. *Eur Neurol* **44**, 236-241.
[43] Rösler M, Anand R, Cicin-Sain A, Gauthier S, Agid Y, Dal-Bianco P, Stähelin HB, Hartman R, Gharabawi M (1999) Efficacy and safety of rivastigmine in patients with Alzheimer's disease: International randomised controlled trial. *BMJ* **318**, 633-638.
[44] Kumar V, Anand R, Messina J, Hartman R, Veach J (2000) An efficacy and safety analysis of Exelon in Alzheimer's disease patients with concurrent vascular risk factors. *Eur J Neurol* **7**, 159-169.
[45] Anand R, Hartman R, Sohn H, Danyluk J, Graham SM (2003) Impact of study design and patient population on outcomes from cholinesterase inhibitor trials. *Am J Geriatr Psychiatry* **11**, 160-168.
[46] Wilkinson D, Schindler R, Schwam E, Waldemar G, Jones RW, Gauthier S, Lopez OL, Cummings J, Xu Y, Feldman HH (2009) Effectiveness of donepezil in reducing clinical worsening in patients with mild-to-moderate Alzheimer's disease. *Dement Geriatr Cogn Disord* **28**, 244-251.
[47] Brassen S, Adler G (2003) Short-term effects of acetylcholinesterase inhibitor treatment on EEG and memory performance in Alzheimer patients: An open, controlled trial. *Pharmacopsychiatry* **36**, 304-308.
[48] Onofrj M, Thomas A, Iacono D, Luciano AL, Di Iorio A (2003) The effects of a cholinesterase inhibitor are prominent in patients with fluctuating cognition: A part 3 study of the main mechanism of cholinesterase inhibitors in dementia. *Clin Neuropharmacol* **26**, 239-251.
[49] Coben LA, Danziger W, Storandt M (1985) A longitudinal EEG study of mild senile dementia of Alzheimer type: Changes at 1 year and at 2.5 years. *Electroencephalogr Clin Neurophysiol* **61**, 101-112.

[50] Soininen H, Partanen J, Laulumaa V, Helkala EL, Laakso M, Riekkinen PJ (1989) Longitudinal EEG spectral analysis in early stage of Alzheimer's disease. *Electroencephalogr Clin Neurophysiol* **72**, 290-297.

[51] Jelic V, Johansson SE, Almkvist O, Shigeta M, Julin P, Nordberg A, Winblad B, Wahlund LO (2000) Quantitative electroencephalography in mild cognitive impairment: Longitudinal changes and possible prediction of Alzheimer's disease. *Neurobiol Aging* **21**, 533-540.

[52] Jewett DL, Zhang Z (1995) Multiple-generator errors are unavoidable under model misspecification. *Electroencephalogr Clin Neurophysiol* **95**, 135-142.

[53] Pascual-Marqui RD, Michel CM (1994) LORETA (low resolution brain electromagnetic tomography): New authentic 3D functional images of the brain. *ISBET Newsletter ISSN* **5**, 4-8.

[54] Talairach J, Tournoux P (1988) *Co-Planar Stereotaxic Atlas of the Human Brain*, Thieme, Stuttgart.

[55] Babiloni C, Binetti G, Cassetta E, Cerboneschi D, Dal Forno G, Del Percio C, Ferreri F, Ferri R, Lanuzza B, Miniussi C, Moretti DV, Nobili F, Pascual-Marqui RD, Rodriguez G, Romani GL, Salinari S, Tecchio F, Vitali P, Zanetti O, Zappasodi F, Rossini PM (2004) Mapping distributed sources of cortical rhythms in mild Alzheimer's disease. A multicentric EEG study. *Neuroimage* **22**, 57-67.

[56] Babiloni C, Benussi L, Binetti G, Bosco P, Busonero G, Cesaretti S, Dal Forno G, Del Percio C, Ferri R, Frisoni G, Ghidoni R, Rodriguez G, Squitti R, Rossini PM (2006) Genotype (cystatin C) and EEG phenotype in Alzheimer disease and mild cognitive impairment: A multicentric study. *Neuroimage* **29**, 948-964.

[57] Babiloni C, Benussi L, Binetti G, Cassetta E, Dal Forno G, Del Percio C, Ferreri F, Ferri R, Frisoni G, Ghidoni R, Miniussi C, Rodriguez G, Romani GL, Squitti R, Ventriglia MC, Rossini PM (2006) Apolipoprotein E and alpha brain rhythms in mild cognitive impairment: A multicentric EEG study. *Ann Neurol* **59**, 323-334.

[58] Babiloni C, Frisoni G, Steriade M, Bresciani L, Binetti G, Del Percio C, Geroldi C, Miniussi C, Nobili F, Rodriguez G, Zappasodi F, Carfagna T, Rossini PM (2006) Frontal white matter volume and delta EEG sources negatively correlate in awake subjects with mild cognitive impairment and Alzheimer's disease. *Clin Neurophysiol* **117**, 1113-1129.

[59] Babiloni C, Cassetta E, Dal Forno G, Del Percio C, Ferreri F, Ferri R, Lanuzza B, Miniussi C, Moretti DV, Nobili F, Pascual-Marqui RD, Rodriguez G, Romani LG, Salinari S, Zanetti O, Rossini PM (2006) Donepezil effects on sources of cortical rhythms in mild Alzheimer's disease: Responders vs. non-responders. *Neuroimage* **31**, 1650-1665.

[60] Babiloni C, Bosco P, Ghidoni R, Del Percio C, Squitti R, Binetti G, Benussi L, Ferri R, Frisoni G, Lanuzza B, Cassetta E, Anello G, Gurzì M, Bartesaghi S, Lizio R, Tombini M, Rossini PM (2007) Homocysteine and electroencephalographic rhythms in Alzheimer disease: A multicentric study. *Neuroscience* **145**, 942-954.

[61] Babiloni C, Bosco P, Ghidoni R, Del Percio C, Squitti R, Binetti G, Benussi L, Ferri R, Frisoni G, Lanuzza B, Cassetta E, Anello G, Gurzi M, Bartesaghi S, Lizio R, Tombini M, Rossini PM (2007) Homocysteine and electroencephalographic rhythms in Alzheimer disease: A multicentric study. *Neuroscience* **145**, 942-954.

[62] Babiloni C, Frisoni GB, Pievani M, Toscano L, Del Percio C, Geroldi C, Eusebi F, Miniussi C, Rossini PM (2008) White-matter vascular lesions correlate with alpha EEG sources in mild cognitive impairment. *Neuropsychologia* **46**, 1707-1720.

[63] Babiloni C, Frisoni GB, Pievani M, Vecchio F, Infarinato F, Geroldi C, Salinari S, Ferri R, Fracassi C, Eusebi F, Rossini PM (2008) White matter vascular lesions are related to parietal-to-frontal coupling of EEG rhythms in mild cognitive impairment. *Hum Brain Mapp* **29**, 1355-1367.

[64] Babiloni C, Frisoni G, Pievani M, Vecchio F, Lizio R, Buttiglione M, Geroldi C, Fracassi C, Eusebi F, Ferri R, Rossini PM (2009) Hippocampal volume and cortical sources of EEG alpha rhythms in mild cognitive impairment and Alzheimer disease. *Neuroimage* **44**, 123-135.

[65] Babiloni C, Pievani M, Vecchio F, Geroldi C, Eusebi F, Fracassi C, Fletcher E, De Carli C, Boccardi M, Rossini PM, Frisoni GB (2009) White-matter lesions along the cholinergic tracts are related to cortical sources of EEG rhythms in amnesic mild cognitive impairment. *Hum Brain Mapp* **30**, 1431-1443.

[66] Babiloni C, Visser PJ, Frisoni G, De Deyn PP, Bresciani L, Jelic V, Nagels G, Rodriguez G, Rossini PM, Vecchio F, Colombo D, Verhey F, Wahlund LO, Nobili F (2010) Cortical sources of resting EEG rhythms in mild cognitive impairment and subjective memory complaint. *Neurobiol Aging* **31**, 1787-1798.

[67] Babiloni C, Frisoni GB, Vecchio F, Pievani M, Geroldi C, De Carli C, Ferri R, Vernieri F, Lizio R, Rossini PM (2010) Global functional coupling of resting EEG rhythms is related to white-matter lesions along the cholinergic tracts in subjects with amnesic mild cognitive impairment. *J Alzheimers Dis* **19**, 859-871.

[68] Babiloni C, Lizio R, Carducci F, Vecchio F, Redolfi A, Marino S, Tedeschi G, Montella P, Guizzaro A, Esposito F, Bozzao A, Giubilei F, Orzi F, Quattrocchi CC, Soricelli A, Salvatore E, Baglieri A, Bramanti P, Cavedo E, Ferri R, Cosentino F, Ferrara M, Mundi C, Grilli G, Pugliese S, Gerardi G, Parisi L, Vernieri F, Triggiani AI, Pedersen JT, Hårdemark HG, Rossini PM, Frisoni GB (2011) Resting state cortical electroencephalographic rhythms and white matter vascular lesions in subjects with Alzheimer's disease: An Italian multicenter study. *J Alzheimers Dis* **26**, 331-346.

[69] Babiloni C, De Pandis MF, Vecchio F, Buffo P, Sorpresi F, Frisoni GB, Rossini PM (2011) Cortical sources of resting state electroencephalographic rhythms in Parkinson's disease related dementia and Alzheimer's disease. *Clin Neurophysiol* **122**, 2355-2364.

[70] Babiloni C, Frisoni GB, Vecchio F, Lizio R, Pievani M, Geroldi C, Fracassi C, Vernieri F, Rodriguez G, Nobili F, Ferri R, Rossini PM (2011) Stability of clinical condition in mild cognitive impairment is related to cortical sources of alpha rhythms: An electroencephalographic study. *Hum Brain Mapp* **32**, 1916-1931.

[71] Babiloni C, Carducci F, Lizio R, Vecchio F, Baglieri A, Bernardini S, Cavedo E, Bozzao A, Buttinelli C, Esposito F, Giubilei F, Guizzaro A, Marino S, Montella P, Quattrocchi CC, Redolfi A, Soricelli A, Tedeschi G, Ferri R, Rossi-Fedele G, Ursini F, Scrascia F, Vernieri F, Pedersen TJ, Hardemark HG, Rossini PM, Frisoni GB (2012) Resting state cortical electroencephalographic rhythms are related to gray matter volume in subjects with mild cognitive impairment and Alzheimer's disease. *Hum Brain Mapp* 2012 Feb 14.

[72] Gianotti LR, Künig G, Lehmann D, Faber PL, Pascual-Marqui RD, Kochi K, Schreiter-Gasser U (2007) Correlation between disease severity and brain electric

LORETA tomography in Alzheimer's disease. *Clin Neurophysiol* **118**, 186-196.
[73] Folstein MF, Folstein SE, McHugh PR (1975) Mini Mental State': A practical method for grading the cognitive state of patients for clinician. *J Psychiatr Res* **12**, 189-198.
[74] McKhann G, Drachman D, Folstein M, Katzman R, Price D, Stadlan EM (1984) Clinical diagnosis of Alzheimer's disease: Report of the NINCDS-ADRDA Work Group under the auspices of Department of Health and Human Services Task Force on Alzheimer's disease. *Neurology* **34**, 939-944.
[75] Hughes CP, Berg L, Danziger WL, Cohen LA, Martin RL (1982) A new clinical rating scale for the staging of dementia. *Br J Psychiatry* **140**, 1225-1230.
[76] Yesavage JA, Brink TL, Rose TL, Lum O, Huang V, Adey M, Leirer VO (1982-83) Development and validation of a geriatric depression screening scale: A preliminary report. *J Psychiatr Res* **17**, 37-49.
[77] Rosen WG, Terry RD, Fuld PA, Katzman R, Peck A (1980) Pathological verification of ischemic score in differentiation of dementias. *Ann Neurol* **7**, 486-488.
[78] Lawton MP, Brodie EM (1969) Assessment of older people: Self maintaining and instrumental activity of daily living. *J Gerontol* **9**, 179-186.
[79] Buchan RJ, Nagata K, Yokoyama E, Langman P, Yuya H, Hirata Y, Hatazawa J, Kanno I (1997) Regional correlations between the EEG and oxygen metabolism in dementia of Alzheimer's type. *Electroencephalogr Clin Neurophysiol* **103**, 409-417.
[80] Pucci E, Belardinelli N, Cacchio G, Signorino M, Angeleri F (1999) EEG power spectrum differences in early and late onset forms of Alzheimer's disease. *Clin Neurophysiol* **110**, 621-631.
[81] Rodriguez G, Vitali P, De Leo C, De Carli F, Girtler N, Nobili F (2002) Quantitative EEG changes in Alzheimer patients during long-term donepezil therapy. *Neuropsychobiology* **46**, 49-56.
[82] Szelies B, Mielke R, Kessler J, Heiss WD (1999) EEG power changes are related to regional cerebral glucose metabolism in vascular dementia. *Clin Neurophysiol* **110**, 615-620.
[83] Moretti DV, Babiloni F, Carducci F, Cincotti F, Remondini E, Rossini PM, Salinari S, Babiloni C (2003) Computerized processing of EEG-EOG-EMG artifacts for multicentirc studies in EEG oscillations and event-related potentials. *Int J Psychophysiol* **47**, 199-216.
[84] Besthorn C, Zerfass R, Geiger-Kabisch C, Sattel H, Daniel S, Schreiter-Gasser U, Forstl H (1997) Discrimination of Alzheimer's disease and normal aging by EEG data. *Electroencephalogr Clin Neurophysiol* **103**, 241-248.
[85] Chiaramonti R, Muscas GC, Paganini M, Muller TJ, Fallgatter AJ, Versari A, Strik WK (1997) Correlations of topographical EEG features with clinical severity in mild and moderate dementia of Alzheimer type. *Neuropsychobiology* **36**, 153-158.
[86] Jelic V, Shigeta M, Julin P, Almkvist O, Winblad B, Whalund LO (1996) Quantitative electroencephalography power and coherence in Alzheimer's disease and mild cognitive impairment. *Dementia* **7**, 314-323.
[87] Leuchter AF, Cook IA, Newton TF, Dunkin J, Walter DO, Rosenberg Tompson S, Lachenbruch PA, Weiner H (1993) Regional differences in brain electrical activity in dementia: Use of spectral power and spectral ratio measures. *Electroenceph Clin Neurophysiol* **87**, 385-393.
[88] Rodriguez G, Copello F, Nobili F, Vitali P, Perego G, Nobili F (1999) EEG spectral profile to stage Alzheimer's disease. *Clin Neurophysiol* **110**, 1831-1837.
[89] Holschneider DP, Waite JJ, Leuchter AF, Walton NY, Scremin OU (1999) Changes in electrocortical power and coherence in response to the selective cholinergic immunotoxin 192 IgG-saporin. *Exp Brain Res* **126**, 270-280.
[90] Kolev V, Yordanova J, Basar-Eroglu C, Basar E (2002) Age effects on visual EEG responses reveal distinct frontal alpha networks. *Clin Neurophysiol* **113**, 901-910.
[91] Nobili F, Taddei G, Vitali P, Bazzano L, Catsafados E, Mariani G, Rodriguez G (1998) Relationships between 99m Tc-HMPAO ceraspect and quantitative EEG observations in Alzheimer's disease. *Arch Gerontol Geriatr* **6**, 363-368.
[92] Pucci E, Cacchiò G, Angeloni R, Belardinelli N, Nolfe G, Signorino M (1997) Angeleri F EEG spectral analysis Alzheimer's disease and different degenerative dementias. *Arch Gerontol Geriatr* **26**, 283-297.
[93] Klimesch W (1996) Memory processes, brain oscillations and EEG synchronization. *Int J Psychophysiol* **24**, 61-100.
[94] Klimesch W, Doppelmayr M, Pachinger T, Russegger H (1997) Event-related desynchronization in the alpha band and the processing of semantic information. *Brain Res Cogn Brain Res* **6**, 83-94.
[95] Klimesch W, Doppelmayr M, Russegger H, Pachinger T, Schwaiger J (1998) Induced alpha band power changes in the human EEG and attention. *Neurosci Lett* **244**, 73-76.
[96] Szava S, Valdes P, Biscay R, Galan L, Bosch J, Clark I, Jimenez JC (1994) High resolution quantitative EEG analysis. *Brain Topogr* **6**, 211-219.
[97] Pascual-Marqui RD, Lehmann D, Koenig T, Kochi K, Merlo MC, Hell D, Koukkou M (1999) Low resolution brain electromagnetic tomography (LORETA) functional imaging in acute, neuroleptic-naive, firstepisode, productive schizophrenia. *Psychiatry Res* **90**, 169-179.
[98] Pascual-Marqui RD, Esslen M, Kochi K, Lehmann D (2002) Functional imaging with low resolution brain electromagnetic tomography (LORETA): A review. *Methods Find Exp Clin Pharmacol* **24**, 91-95.
[99] Yao D, He B (2001) A self-coherence enhancement algorithm and its application to enhancing three-dimensional source estimation from EEGs. *Ann Biomed Eng* **29**, 1019-1027.
[100] Anderer P, Saletu B, Semlitsch HV, Pascual-Marqui RD (2003) Noninvasive localization of P300 sources in normal aging and ageassociated memory impairment. *Neurobiol Aging* **24**, 463-479.
[101] Anderer P, Saletu B, Saletu-Zyhlarz G, Gruber D, Metka M, Huber J, Pascual-Marqui RD (2004) Brain regions activated during an auditory discrimination task in insomniac postmenopausal patients before and after hormone replacement therapy: Low-resolution brain electromagnetic tomography applied to event-related potentials. *Neuropsychobiology* **49**, 134-153.
[102] Laufer I, Pratt H (2003) Evoked potentials to auditory move ment sensation in duplex perception. *Clin Neurophysiol* **114**, 1316-1331.
[103] Mulert C, Gallinat J, Pascual-Marqui R, Dorn H, Frick K, Schlattmann P, Mientus S, Herrmann WM, Winterer G (2001) Reduced event-related current density in the anterior cingulate cortex in schizophrenia. *Neuroimage* **13**, 589-600.
[104] Talairach J, Tournoux P (1988) Co-Planar Stereotaxic Atlas of the Human Brain. Stuttgart: Thieme. AQ4.
[105] Nuwer MR (1988) Quantitative EEG. I: Techniques and problems of frequency analysis and topographic mapping. *J Clin Neurophysiol* **5**, 1-43.

[106] Hernández JL, Valdés P, Biscay R, Virues T, Szava S, Bosch J, Riquenes A, Clark I (1994) A global scale factor in brain topography. *Int J Neurosci* **76**, 267-278.

[107] Rossini PM, Del Percio C, Pasqualetti P, Cassetta E, Binetti G, Dal Forno F, Ferreri F, Frisoni G, Chiovenda P, Miniussi C, Parisi L, Tombini M, Vecchio F, Babiloni C (2006) Conversion from mild cognitive impairment to Alzheimer's disease is predicted by sources and coherence of brain electroencephalography rhythms. *Neuroscience* **143**, 793-803.

[108] Steriade M (2003) Cerebello-cerebral interactions during states of vigilance. *Cerebellum* **2**, 82-83.

[109] Gloor P, Ball G, Schaul N (1977) Brain lesions that produce delta waves in the EEG. *Neurology* **27**, 326-333.

[110] D'Amelio M, Rossini PM (2012) Brain excitability and connectivity of neuronal assemblies in Alzheimer's disease: From animal models to human findings. *Prog Neurobiol* **99**, 42-60.

[111] Pfurtscheller G, Lopez da Silva F (1999) Event-related EEG/MEG synchronization and desynchronization: Basic principles. *Clin Neurophysiol* **110**, 1842-1857.

[112] Hughes SW, Crunelli V (2005) Thalamic mechanisms of EEG alpha rhythms and their pathological implications. *Neuroscientist* **11**, 357-372.

[113] Lorincz ML, Kékesi KA, Juhász G, Crunelli V, Hughes SW (2009) Temporal framing of thalamic relay-mode firing by phasic inhibition during the alpha rhythm. *Neuron* **63**, 683-696.

[114] Capizzano AA, Ación L, Bekinschtein T, Furman M, Gomila H, Martínez A, Mizrahi R, Starkstein SE (2004) White matter hyperintensities are significantly associated with cortical atrophy in Alzheimer's disease. *J Neurol Neurosurg Psychiatry* **75**, 822-827.

[115] Gootjes L, Teipel SJ, Zebuhr Y, Schwarz R, Leinsinger G, Scheltens P, Möller HJ, Hampel H (2004) Regional distribution of white matter hyperintensities in vascular dementia, Alzheimer's disease and healthy aging. *Dement Geriatr Cogn Disord* **18**, 180-188.

[116] Tullberg M, Fletcher E, DeCarli C, Mungas D, Reed BR, Harvey DJ, Weiner MW, Chui HC, Jagust WJ (2004) White matter lesions impair frontal lobe function regardless of their location. *Neurology* **63**, 246-253.